

# Back-Action Evading Measurements on a Trampoline Resonator

#### **THESIS**

submitted in partial fulfillment of the requirements for the degree of

BACHELOR OF SCIENCE in PHYSICS

Author: Camiel van Efferen

Student ID: 1173219

Supervisor : Gesa Welker, Michiel de Dood, Dirk Bouwmeester  $2^{nd}$  corrector : Peter Gast

Leiden, The Netherlands, July 13, 2016

# Back-Action Evading Measurements on a Trampoline Resonator

#### Camiel van Efferen

Huygens-Kamerlingh Onnes Laboratory, Leiden University P.O. Box 9500, 2300 RA Leiden, The Netherlands

July 13, 2016

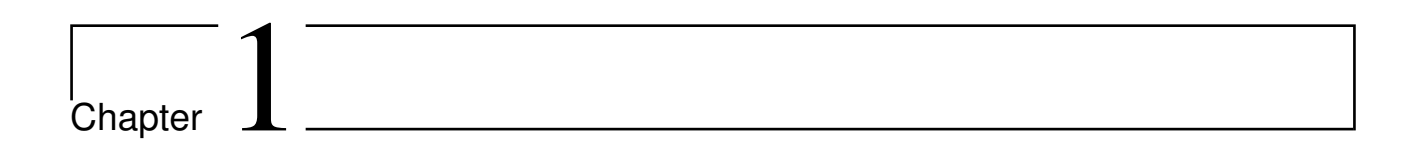
#### **Abstract**

Using an optical cavity, coupled to a micromechanical oscillator - a relatively heavy mass, double trampoline resonator - we will test whether we can, using the method proposed by Clerk *et al.* (2008), perform back-action evading measurements (BAE) in the optical domain on a single quadrature of the oscillator's motion. We will do so by probing the oscillators motion with two optical drives spaced one mechanical resonance frequency above and below the cavity resonance frequency. We will then inject noise in the cavity and analyze the light leaving the cavity. This is intended to show that we can perform classical back-action evading measurements. The long term goal of this project is to find out if this system is capable of reaching or exceeding the standard quantum limit (SQL).

Keywords: BAE, BACK-ACTION, CAVITY, SQL, STANDARD QUANTUM LIMIT, HARMONIC OSCILLATOR, TRAMPOLINE RESONATOR, SIDEBANDS

# Contents

1 I	Introduction	7	
2 (	Goal, Purpose and Structure of this Thesis	9	
3 3 3 3	Setup 3.1 Bragg Mirror 3.2 Cavity 3.3 Trampoline Resonator 3.4 Optical Bench 3.5 Optical Table 3.6 Feedback	11 11 12 14 16 18	
4 4 4 4	Theory 4.1 Cooling 4.2 The Standard Quantum Limit 4.3 Back-Action Evasion: Heisenberg Picture 4.4 The Hamiltonian 4.5 Back-Action Evasion: Wave Picture 4.6 Power Spectral Density and Noise	23 23 25 26 31 34 36	
5 5 5 5	Results 5.1 Finesse 5.2 Quality 5.3 Amplitude Modulation 5.4 Noise 5.5 Analysis 5.6 The Next Steps	39 39 42 45 50 52 60	
6 (	Conclusion	63	
7 A	Acknowledgments	65	
8 8	Appendix  8.1 Appendix 1: Alignment of the Cavity  8.2 Appendix 2: Complete Setup  8.3 Appendix 3: Sample Plane and Mirror	<b>67</b> 67 70 71	



## Introduction

One of the most fascinating and yet frustrating aspects of quantum mechanics is the uncertainty principle, which comes up in many forms, linking variables in a reciprocal bond from which there is apparently no escape: to better see one is always to lose sight of the other. This would not be so great a problem for the experimental physicist however, since it suggests that we can at least know one variable with arbitrary precision. But some of the variables he/she is most interested in, are not so kind: not long after their counterpart has disappeared from view, it returns to disturb the variable you saw so clearly. In this way, all systems have an upper bound to the precision wherewith one can measure their variables.

But in the period between 1970 and 1980 papers began to get published, dealing with the problem of how to detect a gravitational wave [1]. The force exerted by the gravitational wave is so small that to measure e.g. the change it causes in the distance between two harmonic oscillators, one would have to measure the displacement of the oscillator so accurately that the resulting uncertainty in momentum, after one has measured its position, would, by the time one makes a second measurement (after the wave has passed), have caused an uncertainty in the position larger than the effect of the wave [2]. Since the uncertainty principle is a fundamental property of the observables themselves (they do not commute), and not of a certain experimental setup, there seems to be no way around it. But not all observables influence each other like the position and momentum of an harmonic oscillator: some can be measured as precise as one would like, with all the uncertainty dumped in its conjugate observable; these observables we call quantum non-demolition (QND) or back-action evading (BAE) observables [3]. If one could find such an observable for the harmonic oscillator, still carrying the information that we need to calculate the external force that acts upon the oscillator, we open up a realm of investigation that before had seemed hermetically sealed by Heisenberg.

Such observables have indeed been found, and all sorts of BAE evasion measurements were suggested, several of which proved viable for experimental tests [3]. But no one as of yet has succeeded in doing this with our method in the optical domain. We aim to be the first to do this, using a harmonic oscillator with a relatively large mass, making it a distinctly macroscopic object. This is important, for if we want to understand the behavior of macroscopic quantum systems, it would help if we were able to perform continuous measurements of such a system in isolation; this is what our BAE scheme would provide us with.



# Goal, Purpose and Structure of this Thesis

If a thing is small enough, it just can't stop itself from behaving quantum. To show that electrons tunnel through potential barriers, or prove that photons are sometimes created in entangled pairs currently is very easy, certainly when you compare it to trying to catch a macroscopic object in a quantum state. The larger the object, the less we observe quantum behavior. But there is nothing in quantum mechanics which predicts that it is actually impossible for large objects to do this, provided that they are sufficiently isolated from their environment. If we could prepare such objects, an interesting possibility would be to use such objects to study decoherence under the influence of gravity [4]. But since quantum mechanical behaviour takes place on such a small scale, one would like to measure very accurately and this is problematic. No matter how well you measure it, any continuous linear measurement of the position of a mechanical oscillator masks its quantum behaviour [5]: the effect of your measurement being larger than the effect one would like to measure. This is the background of my project: the long term goal of the Bouwmeester group to entangle a macroscopic object with a photon to study superpositions, entanglement and decoherence of macroscopic objects, and the PhD project of Gesa Welker to design a setup capable of measuring so accurately that this results in a quantum squeezed state of the mirror [5].

For my Bachelor's project, we want to find out if we can create an experimental setup, using the double trampoline resonator of the Bouwmeester group [6], that can in principle be used for BAE measurements. Since we know what kind of materials and physical parameters we are dealing with, we know that it should be possible to do classical BAE measurements. Our goal is thus to realize an actual setup able to perform such measurements. We check whether this has succeeded by injecting noise into a Fabry-Pérot cavity, of which the trampoline resonator is the back-mirror, driven with two optical drives spaced above and below the cavity resonance frequency by exactly the mirror resonance frequency. We then see whether our measurement of a single quadrature of motion of the resonator is disturbed by the noise. This shows that we evade the back-action on our mirror which arises from this classical noise. We can then try to improve upon our design, seeking to delve below the SQL, the limit that results from Heisenberg's uncertainty principle. At this point the back-action will be generated by the shot noise of our measurement beam.

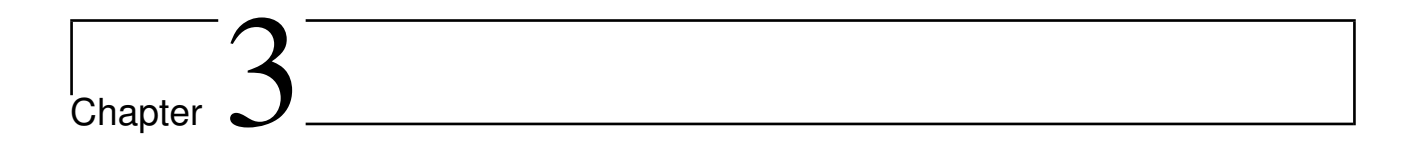
No one has before performed BAE measurements in the optical domain, we aim to be the first; and knowing that our system is sideband resolved we are confident that we can at least perform classical BAE. We seek to put into practice the theory provided by Clerk *et al* (2008) and create an experimental setup that can in principle be used to measure very weak forces, beyond the limits imposed by back-action noise. We will do this through measurements of a

single quadrature of the mirror's motion. Our system is unique in that its oscillator consists of two resonators, providing excellent vibration shielding from the environment, and has a particularly large mass, which might allow eventual study of the decoherence of macroscopic objects.

I will first treat the most important elements our setup consists of, and at the same time present the theory behind the optomechanical coupling of the mirror to the light circulating the cavity. I will then give a more theoretical and detailed explanation of the quantum mechanics of optomechanical cooling and back-action evasion. The theoretic part of the thesis will end with a discussion of the Hamiltonian describing the interaction between our measurement system and the observable we measure and the power spectral densities of the noise we can expect given certain conditions. The last chapter will deal with the results. I will explain some of the preliminary tests we have performed to check whether our sample was adequate and provide proofs that our methods of creating sidebands and noise are functional. The chapter ends with a analysis of the results of our first measurements and a glance at the future of this project.

Table 2.1: Overview of the most important symbols used in this thesis.

Symbol	Meaning
$\omega_c$	Cavity resonance frequency
$\omega_l$	Laser frequency
$\omega_{fsr}$	Free spectral range of the cavity
$\omega_{aom}$	Modulation frequency of the AOMs
Δ	Cavity detuning $(\omega_l - \omega_c)$
$\Omega_m$	Mechanical resonance frequency
$\kappa$	Linewidth of the cavity
$ au_c$	Lifetime of a photon in the cavity
$ au_c$ $F$	Finesse of the cavity
L	Cavity length
G	Optical frequency shift per displacement
Q	Mechanical quality factor
$\gamma_m$	Linewidth mechanical oscillator
$\hat{X}_1, \hat{X}_2$	Real and imaginary part of the complex amplitude of the oscillator; quadratures
T, R	Transmitivity and Reflectivity of the mirrors.



Our setup consists of three parts: two on the optical table and one in a vacuum chamber. The part that goes into the chamber is our optical bench, which is essentially a massive block of aluminum designed to minimize vibrations, with placeholders for mirrors, a photodetector, a fiber and two lenses. We form an optical cavity of two not perfectly reflective Bragg mirrors, and use two regular mirrors to form a periscope allowing us to direct the light to the middle of both mirrors. Right after the fiber we place a lens, which allows us to collimate the light; another lens is placed before the first Bragg mirror to mode-match the light to the cavity. Behind the cavity then, a photodetector is fastened, so we can measure the intensity of the light transmitted through the cavity.

This chapter will begin by explaining the theory behind the more important parts of this setup. This will also enable me to introduce some concepts which I will later make use of in the theoretical section. Since coming up with a good design for the optical bench was the first part of this project, I also start here. We then move to the optical table, where we had to build a light path that creates the two optical drives. I will from now on refer to these optical drives as sidebands. I will end with a discussion of the third part: the feedback system which keeps our laser beam at the right frequency.

### 3.1 Bragg Mirror

The Bragg mirrors which make up our cavity make a good starting point for explaining the cavity itself. A Bragg reflector mirror consists of layers of materials with different refractive indices. Let's say we want to construct a mirror with maximum reflectivity for a certain wavelength. We would then use a stacking of layers which makes certain that under normal incidence the reflected rays all constructively interfere with each other. The way this is usually done, is by stacking layers of material, all with an optical thickness  $\frac{\lambda}{4}$  (optical thickness = refractive index × geometrical thickness), but with alternating refractive indexes, on each other so that light of wavelength  $\lambda$  is optimally reflected. To understand this we need to know that when light is reflected traveling from a lower to higher index material it gains a  $180^{\circ}(\pi)$  phase shift. So when we start with a high index material the light traveling to the air will be reflected with a  $180^{\circ}$  phase shift, but the transmitted light which is later reflected traveling through the high index material to the second layer of lower index is not phase shifted because of reflection. Instead it has traveled an optical path length of twice  $\frac{\lambda}{4}$ , which means that when it is transmitted back to the air it also is phase shifted by  $\frac{\lambda}{2} = 180^{\circ}$  relative to the incoming light. The same holds for the next two layers etc. By stacking these pairs of

layers we can achieve almost total reflection at a certain wavelength. But some of the light still enters the cavity. Since our mirrors are two-sided, they will reflect the light in the cavity in the same way. Therefore there are an uneven amount of layers in each mirror (so that they are symmetric). And if the cavity has length  $m\frac{\lambda}{2}$ , with m any integer, the light that has made one roundtrip through the cavity will have traveled a pathlength of  $m\lambda$  and it has been phase shifted by  $180^{\circ}$  through reflection. This will destructively interfere with the promptly reflected light; the reflected beam can completely vanish in this way. This can be understood when we consider that the light coming from the cavity traveled an additional  $2\frac{\lambda}{4}$  because of the uneven stacking and is thus  $180^{\circ}$  out of phase with the immediately reflected light \*.

#### 3.2 Cavity

The cavity consists of two distributed Bragg reflector mirrors: a large one which for all practical purposes we consider to be at a fixed position, and a much smaller one which is a mechanical oscillator. The distance between the two mirrors (we take the equilibrium position of the vibrating mirror) is fixed so that it is an half-integer multiple of the wavelength  $\lambda$  of the laser that enters the cavity through the large mirror. Since the mirrors are  $\frac{\lambda}{4}$  distributed Bragg reflector mirrors we have in this way created a perfect 'trap' for the light that enters the cavity. The mirrors are almost perfectly reflective for  $\lambda^{\dagger}$  and the distance  $\frac{1}{2}m\lambda$  is chosen so, with m any integer, that a wave will fit an integer number of times in a round trip through the cavity, so that it will not destructively interfere with the incoming light. Once it has reached the input mirror it will be phase shifted by  $2m\pi$  and is thus in phase with the incoming light. The cavity thus has a certain resonance frequency  $\omega_c$ , meaning it is maximally attuned to light of frequency

$$m \cdot \pi \frac{c}{I} \tag{3.1}$$

with m the integer mode number [7]. We can also consider that therefore  $\pi_L^c$  denotes the distance between two resonant frequencies, which is called the free spectral range of the cavity  $\Delta \omega_{fsr}$ . Since it does not matter which frequency light has for the time it takes for light to travel between the two mirrors, we can quantify for all resonant modes the finesse of the cavity:

$$F \equiv \frac{\Delta \omega_{fsr}}{\kappa} \tag{3.2}$$

with  $\kappa$  the full width at half maximum (FWHM) of the bandwidth of the cavity, or the inverse of the lifetime  $\tau_c$  - the decay rate - of a photon in the cavity. F thus denotes the average amount of roundtrips a photon makes before it leaves the cavity [7].  $\kappa$  gives the FWHM of a lorentzian peak around the cavity resonance. It denotes the transmitivity of the cavity for different frequencies of light, with a maximum at the cavity resonance frequency. It is dependent on the reflectivity of the mirrors, the length of the cavity and how well aligned the cavity is. The theory behind the finesse and the linewidth can be found in section 5.1. The practice of alignment is discussed in sections 3.4 and 8.1.

Now we let the back-end mirror oscillate - in the case that no light enters the cavity yet -

<sup>\*</sup>We can imagine the cavity as a  $\frac{\lambda}{2}$  layer of low refractive index in a Bragg mirror where there should be a  $\frac{\lambda}{4}$  layer. But you don't have to use Bragg mirrors to make a cavity. You can also make one e.g. with a plate of any refractive index having two reflective surfaces, as long as its thickness is  $m\frac{\lambda}{2}$ , the light transmitted back from the cavity to the incoming beam will destructively interfere with the promptly reflected light.

<sup>&</sup>lt;sup>†</sup>In our case  $\lambda = 1064$  nm, all our mirrors and fibers are attuned to this wavelength.

3.2 Cavity 13

as the result of the Brownian motion of the atoms it consists of. It has around three times its number of atoms of normal modes of vibrations, which makes up quite a large number; but it mainly oscillates in its fundamental mode  $\Omega_m$ , which is to a great degree decoupled from all other modes [1]. When we drive the oscillator in this mode for a time and then stop, its energy decreases through destructive interference with the other modes. The number of radians of oscillation required for its energy to decrease by 1/e is its quality factor Q, which is thus a measurement for the degree of decoupling from the other modes [1]. As the mirror oscillates - we assume at only its fundamental mode  $\Omega_m$  - the cavity length changes and with the length changes the resonance frequency of the cavity. If we now turn on the laser, and shine light in the cavity, the amount of photons circulating in the cavity changes as the mirror oscillates.

We can now define an optical frequency shift per displacement caused by the mirror's deviations from the equilibrium position x=0 as  $G=-\partial \omega_c/\partial x|_{x=0}$ , which for a simple cavity  $(\omega_c=m\cdot\pi(c/L))$ , is easily calculated to be:

$$G = \omega_c / L \tag{3.3}$$

But the dynamics of the cavity do not just consist of the dependence of the amount of photons on the mirror's displacement, since photons carry a momentum  $\hbar\omega_c/c$  with  $\hbar$  Planck's reduced constant,  $\omega_c$  the angular frequency of the light resonant with the cavity and c the speed of light. Now when a certain amount of photons circulates in the cavity, we can calculate the total momentum imparted on the mirror each second, arriving at the force that is exerted by the light on the mirror. A simple calculation delivers:

$$F = \hat{a}^{\dagger} \hat{a} \cdot (2\hbar\omega_c/c)/\tau_p = \hbar G \hat{a}^{\dagger} \hat{a}$$
 (3.4)

with  $\tau_p = 2L/c$  the time it takes for a photon to make a roundtrip, and the momentum per photon doubled, because the momentum imparted upon reflection is twice as large as the photon momentum due to the reversal of direction, and the amount of photons given by the product of the creation and annihilation operators for the field inside the cavity  $\hat{a}^{\dagger}\hat{a}$ , which has the number of photons in the cavity as expectation value.

This force, being dependent on the amount of photons in the cavity and the cavity length, will necessarily fluctuate while the mirror moves, but it will also cause a static displacement of the mirror's equilibrium position. So we define the average value of the light field in the cavity:

$$\bar{a} = \hat{a} - \hat{d} \tag{3.5}$$

with  $\hat{d}$  the fluctuating part of the light field as the result of both the mirror motion and the vacuum fluctuations, so that  $|\bar{a}|^2 = \bar{a}^\dagger \bar{a}$ , which is the average amount of photons in the cavity at each moment. Our average force arising from radiation pressure becomes:

$$F = \hbar G |\bar{a}|^2 \tag{3.6}$$

If we want to calculate how much the equilibrium is displaced as the result of this force, we use the regular expression for the motion of the oscillator, remove all time derivatives and keep:

$$\partial x = F/m_{eff}\Omega_m \tag{3.7}$$

With  $m_{eff}$  the effective mass of the mirror. All this implies of course that L has increased, so that the cavity resonance frequency has shifted, and we need to adjust our laser accordingly, by detuning it by an amount  $G\partial x$ , so that it is again resonant [7]. I will return later to the fluctuating terms of the force; this section has dealt with the 'static' part of the dynamics of the interaction between the mirror and the light.

#### 3.3 Trampoline Resonator

If we want to precisely measure the influence of light on the mirror, it needs to have both a small mass - so it is more easily displaced by radiation pressure - and to be isolated from vibrations from the environment - so we can actually measure the role of light. In our case however, the mirror has a relatively large mass, because it is designed to ultimately perform in tests for quantum superpositions in large mass systems [6]. I will not consider in this section the details of production which can be found in reference [6] and only discuss its shape and the parameters we can realize using it. Of crucial importance is to show that we can build a side band resolved system with it ( $\kappa \ll \Omega_m$ ), the role of which will be discussed in further sections.

As we can see in Fig 3.1, the resonator consists of two parts: a small Bragg mirror in the middle, connected with four arms to a round mass, which is suspended on four thin arms. The inner mirror is the harmonically oscillating end mirror of our cavity, while the outer mass functions as a mechanical low-pass filter, to prevent the coupling of the oscillator to unwanted vibrations.

Concerning the parameters: our trampoline resonator can reportedly be used to create an optical cavity with a finesse F of  $180000 \pm 1000$  [6]. Given that the length L of our cavity is 5 cm and the angular frequency  $\Omega_m$  of the inner resonator  $\approx 2\pi * 250$  kHz [6], we can readily calculate that:

$$\kappa = \pi c / FL \approx 2\pi * 16000 \ll \Omega_m \tag{3.8}$$

Which places us firmly within the sideband resolved regime [7].

Here must however be noted, that during the course of my Bachelor project we used another trampoline resonator. Initially as a test, but when it proved viable to achieve our goals at that time we continued with it, though the project will eventually make use of the double resonator I described above. The second resonator provides excellent vibration isolation and we'll need that when we perform truly sensitive measurements. We used the single resonator of Fig. 3.2. In Appendix 3 I've included pictures taken from our actual sample plan and mirror.

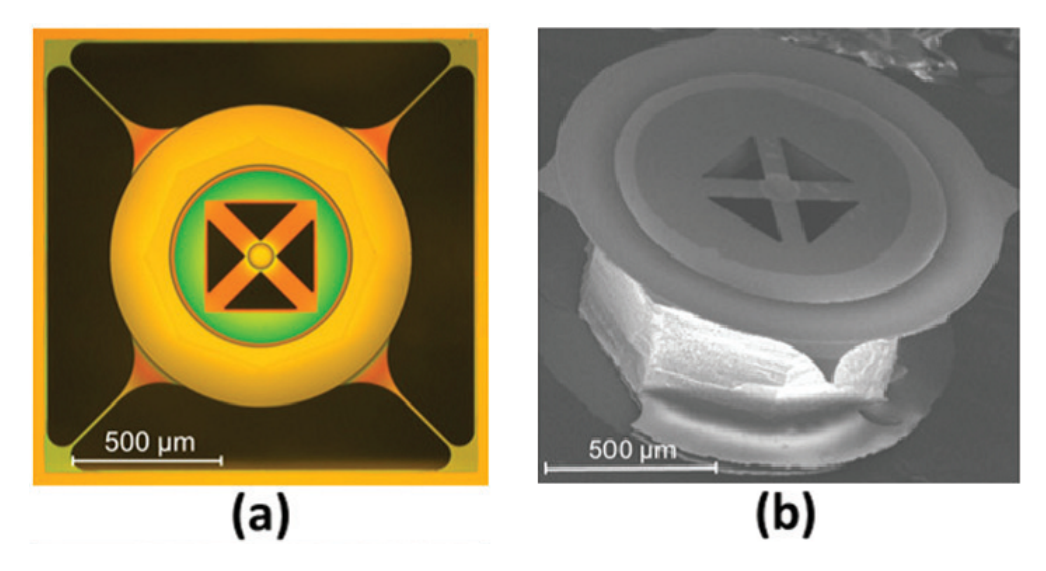


**Figure 3.1:** An optical a) and a SEM b) picture of the trampoline resonator, pictures taken from ref [6].

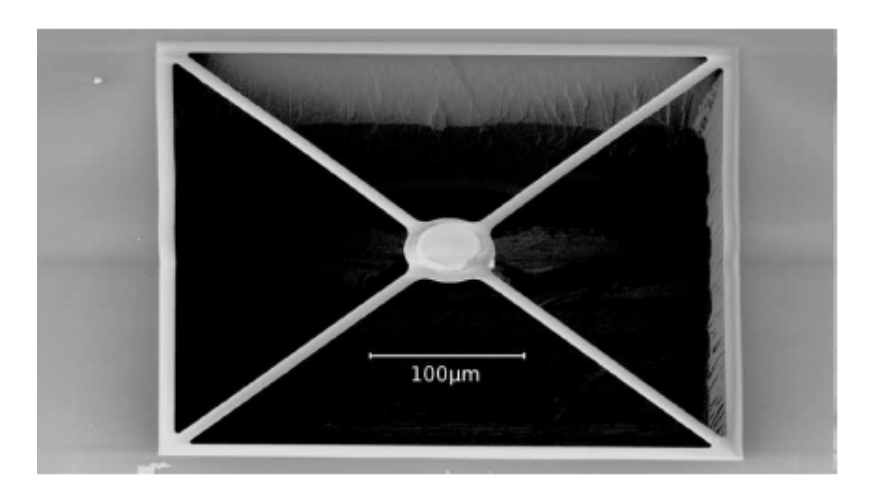


**Figure 3.2:** STM image of the kind of resonator we have used during the course of this Bachelor project. The size of the mirror can vary. Picture taken from ref [8].

### 3.4 Optical Bench

The optical bench we designed needed to fulfill certain criteria, the most important of which were solidity and precision. It needed to be as massive and solid as possible to make sure that we minimized unwanted vibrations which could distort the measurement or the optical path, which needs to be very precisely aligned because the finesse of our cavity would greatly suffer if our incoming laser beam is not tuned to have normal incidence at both the input mirror and the moveable mirror (e.g. the Bragg mirrors would not reflect as much, since the optical path through a layer is larger than  $\frac{\lambda}{4}$  if it does not strike the mirror at normal incidence). So the challenge was to create a design with a minimum of loose or adjustable parts, yet with enough degrees of freedom to make sure the optical path can be precisely aligned. And because a vacuum is required for the measurements we want to perform, the whole setup needed to be vacuum-compatible, placing extra restraint on the materials we could work with.

I'll start with the most important part - the cavity - and then work my way back to the input fiber, through the whole design. The cavity itself consists of two mirrors, divided by a distance L. We need to be able to slightly adjust this distance, because the efficiency of our cavity will rapidly fall, if we cannot make sure that our Bragg mirrors, the wavelength of the laser and the length of the cavity are tuned to the same  $\lambda$ . We also need to be able to adjust for small displacements from the focal point of the lens.

Therefore we need at least the freedom to change L, which requires that we can move at least one of the mirrors in the z-direction. Also we need to be able to align the two mirrors, so that they are facing each other under normal incidence. Therefore we need either one mirror having all five relevant degrees of freedom (x-, y-, z-translation and tip-, tilt rotation), or both having at least rotational freedom, besides the possibility of movement in the z-direction. We need only two rotational degrees of freedom because we use spherical mirrors. This means that rotation around the z-axis would not make any difference and because we try to hit the center anyway, rotation around the z-axis would be doubly senseless for a beam coming at normal incidence from the z-direction. The reason we need both mirrors to have rotational freedom that if one of the mirrors is slightly tilted, we cannot fix this in any way by adjusting the rotation of the other, if it cannot move in the x- and y-direction also. However, if both can be rotated, we can easily imagine how we can make sure that they face each other, whatever the initial positions may be. We chose to be able to move both mirrors, because it would be more difficult to build a vacuum compatible x-, y-translation stage than to emulate standard mirror mounts in the design of the cavity.

Following the light, we come to the question of how to make sure that the light we send into the cavity is nicely aligned with it. We have the same options as before: either we make sure that our light source has five degrees of freedom, or we use two mirrors which can at least tip and tilt to align the light from the source, which can then be fixed. We again chose the second option, installing into the bench two mirror mounts which form a periscope, allowing us to precisely fix the incoming laser beam.

As we arrive at the source of the light, we realize that we cannot simply use a fiber directed at the periscope, as the light coming from a fiber diverges, which, if left unchecked, will have resulted in a spatially incoherent beam when the light finally reaches the cavity. Since it is crucial for our experiment that the light in the cavity consists of only a single mode, we need a lens, collimating the light coming from the input fiber. This lens must be

3.4 Optical Bench 17

able to move in the z-direction, in order to correct for possible misalignment. For this we use an attacube, which can be controlled remotely, giving us a certain measure of control after we've entrusted the setup to the vacuum.

The last piece, which we cannot see in Fig. 3.3, is the photodiode we'll use to measure the light that is transmitted through the cavity. It is placed almost immediately behind the cavity, and is much larger than the beam width actually transmitted.

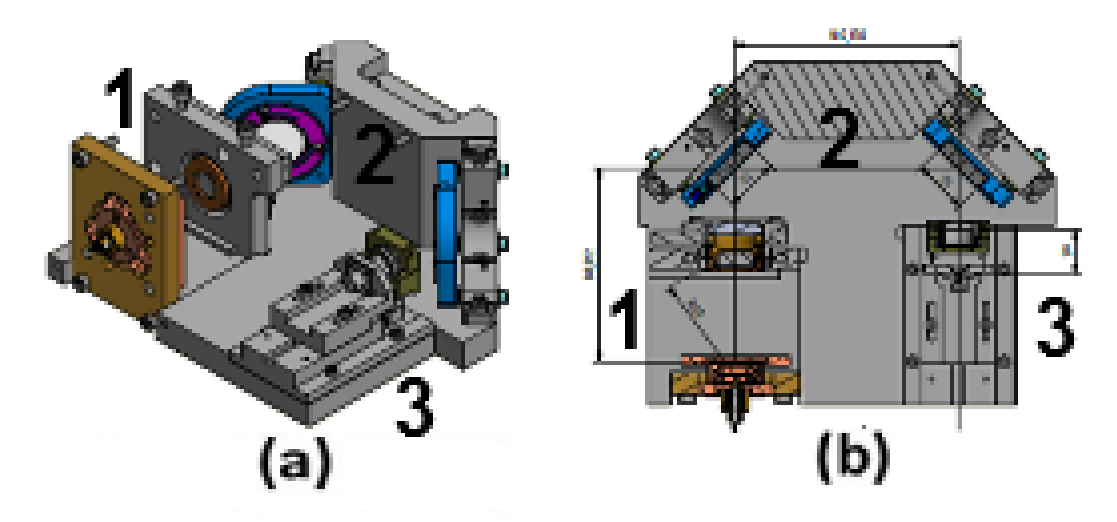


**Figure 3.3:** The optical bench built by Harmen van der Meer of the FMD. Left we see the cavity (1), on the upper side the periscope (2) and on the right the fiber holder and lens (3).

Another important element however, was the fact that the optical bench would need to be capable to function in vacuum. This meant that we had to choose materials for the construction which do not outgas. Outgassing is the evaporation of oils as a result of the lower air density. This oil could cloud the mirrors and ruin our vacuum; so special care was taken to select only vacuum compatible elements. Also we have cleaned all parts of the optical bench in a vibrating bath, once in water with soap and once in propanol, before we put the mirrors and lenses in.

### 3.5 Optical Table

On the optical table we built a path capable of creating the two sidebands out of a laser originally at the cavity resonance frequency. We used acoustic optical modulators (AOMs)<sup>‡</sup> to do this, which made sure that we were also capable of pulsing the laser as required for finesse measurements. I will go through the different elements of the setup and explain their purpose, the actual proofs of the method are given in the chapter which discusses the results of this Bachelor project 5.

The laser that we use for our measurement beam is located in the small optical lab, whereas our setup is in the big optical lab. So the laser is coupled into a fiber in the small lab and coupled into free space again in the big lab. When light exits a fiber, it will diverge, so a lens is placed immediately after the fiber to collimate the beam. The fiber holder and lens are situated on a x-, y-, z-stage. The beam then goes through a  $\lambda/2$  plate, which gives us some control over the polarization. In this way we can determine how much light is transmitted through the polarizing beam splitter (PBS) and eventually to the cavity. Then a lens focuses the beam on the first AOM. Here the light is diffracted into multiple orders and undergoes a frequency shift. A first order beam is selected and focused on the second AOM. This AOM is amplitude modulated so that its first order beam is turned on and off periodically at the modulation frequency. We select the opposite first order beam (so that it is frequency shifted in the opposite direction and back again at the original frequency) and collimate it with a lens. We then use a periscope to mode match the light to a single mode fiber.

The fiber is then joined to another fiber with a 90:10 fiber beam splitter. The other fiber is attached to the Toptica laser, which we use to inject noise in the cavity. We choose the exit port of the fiber beam splitter so that 90% of the measurement light goes through and thus only 10% of the noise power. This exit fiber meets another 90:10 fiber beam splitter. On the other entry port we place a fiber coming from the small optical lab. We send in light used for the feedback lock in this way, and gather the light reflected from the cavity, also for the feedback lock. For this reason 90% of the feedback lock light goes through the cavity: because a fiber beam splitter is symmetric, this means that of the light reflected from the cavity also 90% will go to the small optical lab. The optical bench contains the elements I've already treated.

<sup>&</sup>lt;sup>‡</sup>An AOM consists of a crystal with a piezo element attached to it. The piezo can be expanded and contracted periodically when a voltage is applied to it and in this way causes sound waves to travel through the crystal. The sound waves change the density of the crystal periodically and therefore the refractive index. This creates a Bragg grating from which light can be diffracted. Light that is diffracted is frequency shifted as a result of their interaction with the sound waves by an amount equal to the frequency of the sound waves. Depending on which order, this shift can be positive or negative.

3.6 Feedback 19

#### Big Optical Lab

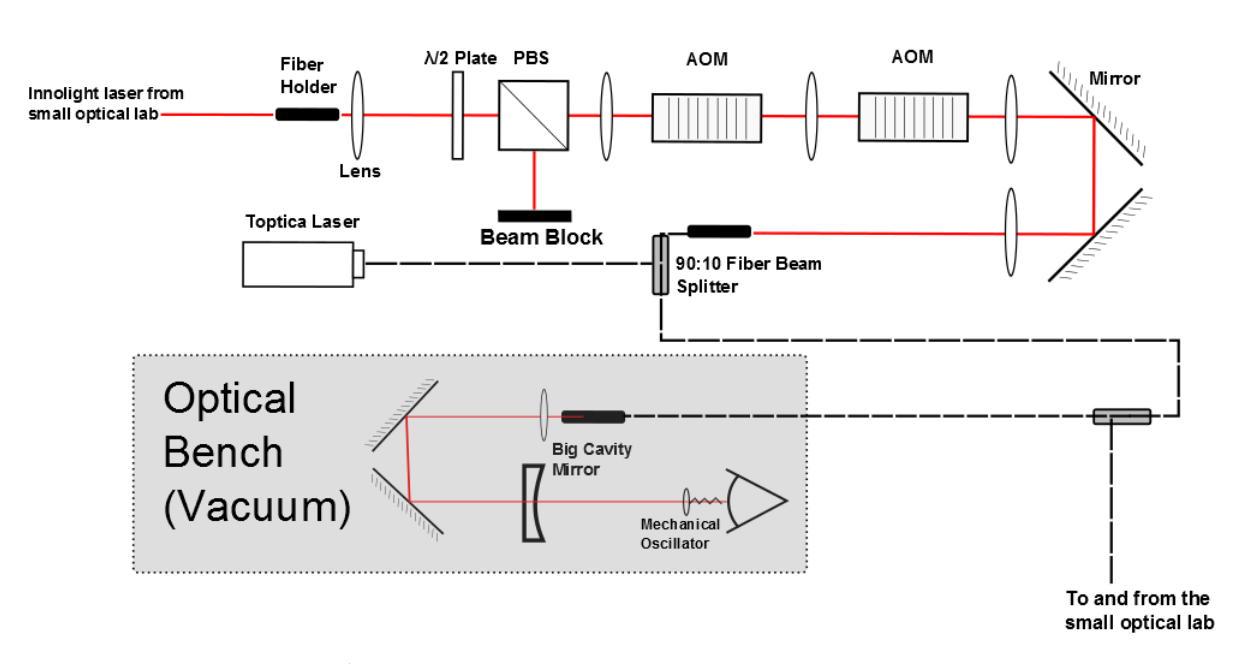


**Figure 3.4:** Schematic of path in the big optical lab and the optical bench. We collimate the beam which comes out of the fiber with a lens. Then we control the polarization of the light leaving the fiber with the  $\lambda/2$  plate, such that we can determine how much enters the cavity through the polarizing beam splitter. We then focus the beam on the first AOM and then again on the second AOM. Then the beam is collimated again and using a periscope we mode match it to a single mode fiber. This fiber is joined by another fiber with a 90:10 beam splitter. This other fiber is used to inject noise coming from the Toptica laser in the cavity. We use the second beam splitter to join the light used for a feedback lock. All are sent to the cavity. The light reflected from the cavity is collected in the small optical lab to be used for the feedback lock.

#### 3.6 Feedback

Whenever someone wants to measure anything accurately, he must make sure that his tool for measuring is stable, at the very least more stable than what he tries to measure with it. Our tool is a laser, but lasers are never completely stable in their frequency output. To make sure that out laser stays at the cavity resonance frequency, we have to implement a feedback loop. The one we use is called Pound-Drever-Hall. I will briefly explain the method and introduce the elements in the small optical lab that we've used to realize it.

In general, the problems you encounter in locking a laser to a cavity are due to the fact that if you want to know if your laser is stable by checking the intensity response of the cavity, you cannot do so at resonance, for it is symmetric there (so that if your laser is tuned to resonance and drifts away you have no way of knowing whether you have drifted to the left or the right of your original position, since in both cases the reflected intensity increases). If you try to measure instead where the intensity slope is steepest, you have something else to deal with: because the laser also fluctuates in intensity, your feedback system cannot distinguish between frequency and intensity fluctuations. The idea of the Pound-Drever-Hall technique is therefore to measure the phase of the reflected light around resonance. The phase of the reflected beam is indeed sensitive to what side of the resonance the laser has drifted to. But we cannot read out the phase of an optical signal with a photodetector. So

something else has to be measured: the beat pattern between the reflected beam and two sidebands, created by phase modulation of the original beam.

The Pound-Drever-Hall technique for optical frequencies uses an electro-optical modulator (EOM) to sinusoidally modify the original frequency of the laser beam which is resonant with the cavity. An EOM is a crystal which, when a voltage is applied to it, periodically changes its refraction index. Light traveling through it can in this way be phase modulated: its instantaneous frequency oscillates. The modulation signal is provided by a local oscillator. The process can be described as:

$$E_0 e^{i\omega_c t} \to E_0 e^{i(\omega_c t + \beta \sin \Omega t)} \tag{3.9}$$

With  $E_0$  the amplitude of the electric field and  $\Omega$  the modulation frequency.  $\Omega$  is chosen so that it is far from cavity resonance (9.55 MHz). Using small angle expansion [9] we can also write this as three beams now incident on the cavity: an original beam of angular frequency  $\omega_c$  and two sidebands at  $\omega_c \pm \Omega$ , with the amplitude of the sidebands much smaller than that of the original beam. The beat pattern between these sidebands and the original beam will oscillate at  $\Omega$  and will differ in phase depending on what side of resonance you're on. But 9.55 MHz is still a very fast oscillation.

So, when these beams reach the cavity, the sidebands will promptly be reflected and the beam near resonance will be more or less reflected depending on how well it resonates with the cavity. All reflected light will be collected by a photodetector. This signal will then be mixed with a signal provided by the same local oscillator that originally provided the modulation signal. A phase shifter is used to make sure that we can adjust for the difference in pathlength between the two signals. Using basic trigonometry:

$$\sin(\Omega t)\sin(\Omega' t) = \frac{1}{2}[\cos((\Omega - \Omega')t) - \cos((\Omega + \Omega')t)]$$
 (3.10)

With  $\Omega'$  the frequency of a local oscillator which is mixed with the signal from the photodetector. If now the local oscillator is the same that we used to create the sidebands, and it delivers the same frequency signal without phase difference  $\Omega = \Omega'$ , then we can use:

$$\sin(\Omega t)^2 = \frac{1}{2} [1 - \cos(2\Omega t)] \tag{3.11}$$

This signal we filter with a low-pass filter to select only the dc component. The phase information is carried by the amplitude of this dc component, and it can be used to create an error signal sensitive to what side of resonance you are on. This is fed to a PID controller which puts the laser back on resonance. Fig. 3.5 is a schematic drawing of the whole PDH setup. For a truly good discussion see Ref. [9].

3.6 Feedback 21

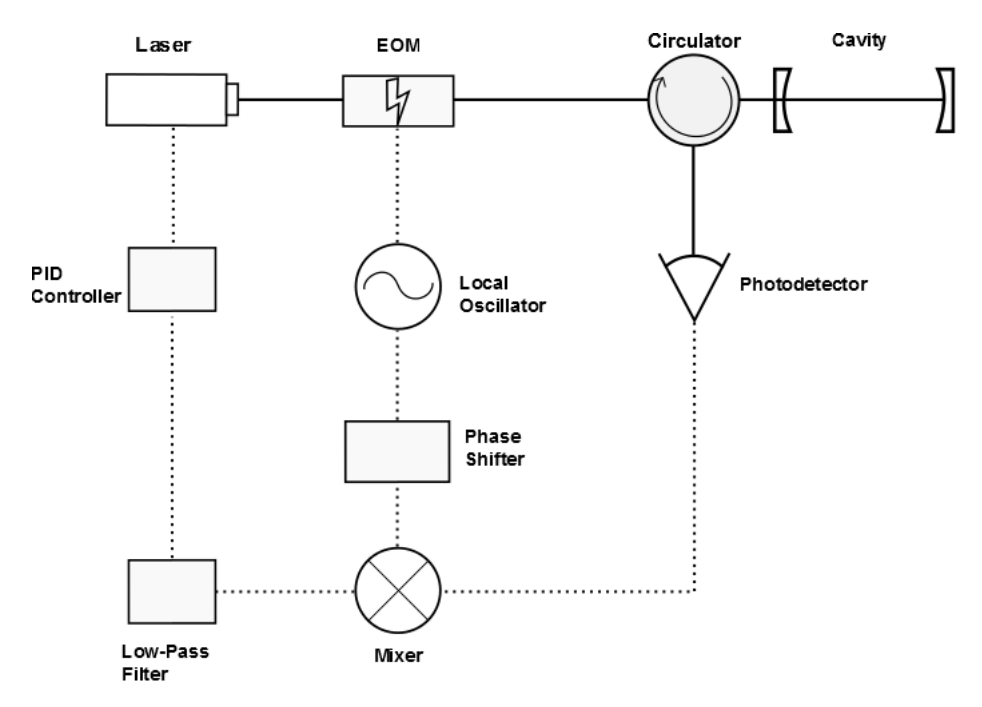
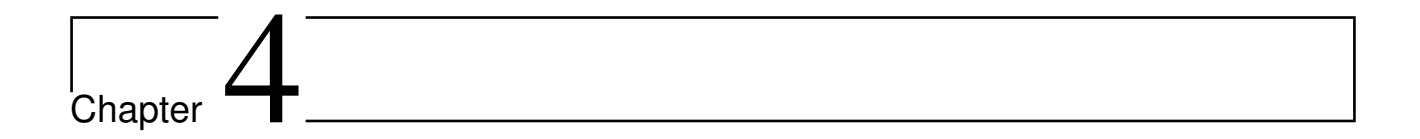


**Figure 3.5:** The original laser beam is modulated by the EOM, so that it gains two sidebands. Then the reflected light is collected by the photodetector, [while the isolators make sure that no light is reflected back to the laser]. The signal from the photodetector is put into the mixer, along with the modulation signal that was previously applied to the EOM. The phase shifter takes care of possible differences in the path length of both signals. The mixer produces an output signal that is a product of the two incoming signals, which contains a dc term. After the signal has passed the low-pass filter, only this dc signal is left. This is fed to the PID controller which alters the laser frequency in response to the signal. Original picture due to Eric D. Black [9].



## 4.1 Cooling

It is possible, using the forces that light exerts on the mirror, to cool or heat it; that is, energy from the mechanical Brownian motion can be turned into electromagnetic energy and vice versa [10]. This happens through a process analogous to Raman scattering [7]. I will explain this process and in this way introduce some of the concepts which are crucial for understanding back-action evasion. During our BAE method the mirror is simultaneously cooled and heated.

Raman scattering is a process where atoms or molecules emit light of a different wavelength than the light that originally excited the transition. Since the emitted photon has a higher or lower frequency than the exciting photon, some energy transfer must have occurred. In the same way we can cool or heat the oscillator, it is called Stokes scattering then [7]. To explain this we need to take into account that the vibrational energy of the mirror is quantized: we can regard the whole mirror as a system of harmonic oscillators, vibrating at the different eigenfrequencies of the normal modes of the system. Each of these harmonic oscillators has a quantized energy of  $(n+\frac{1}{2})\hbar\Omega$ , with  $\Omega$  a mechanical frequency of oscillation and n the number of quanta which are called phonons. But we don't need to consider all these frequencies, for the mirror oscillates at a single normal mode of vibration, which is more or less independent of all the other modes of the mirror. This mode has a certain mean phonon occupation grade  $\bar{n}_m$  and oscillates at the mechanical resonance frequency  $\Omega_m$ .

When light scatters off the mirror, there is a chance that it will interact with these phonons in such a way that a photon of frequency  $\omega$  is absorbed and a photon with  $\omega \pm m\Omega_m$  emitted, with m some integer. This is because as the mirror moves and the cavity resonance frequency changes through Eq. (3.3), it will start to emit photons at frequencies  $(\omega_l \pm j\Omega_m)(j=1,2...)$  any time the cavity resonance is changed to one of these frequencies as a result of the mirror's motion [11]. Since this process is symmetrical, just shining a laserbeam of any frequency on a mirror would neither cool nor heat it. Some photons will be upconverted, taking away m phonons of the mirror, thus cooling it. And the same amount will be down-converted, increasing the vibrational energy of the mirror by exactly  $m\hbar\Omega_m$ . But now we introduce a cavity. The cavity has a certain linewidth  $\kappa$  which places constraints on the wavelength of photons admitted in the cavity.

Let us first assume that  $\kappa > \Omega_m$ . If we use a laser at the cavity resonance frequency  $\omega_c$ , we still have simultaneous heating and cooling in the same way as described above with

the added condition that  $m\Omega_m \ngeq \kappa$ , so that scattering to higher orders is prohibited by the finite cavity linewidth. But if we now move the laser, detuning it to either side of the cavity resonance we introduce an asymmetry in this process.  $\kappa$  was briefly introduced in section 3.2 as denoting the FWHM of the lorentzian peak around the cavity resonance frequency specifying the transmittivity of the cavity for certain frequencies. If light is well outside this peak, it will destructively interfere with itself and cannot enter the cavity. The same goes for light in the cavity interacting with the mirror. If absorbing one phonon of energy from the mirror for instance would create a photon with a wavelength outside the cavity bandwidth, this occurrence is reduced. If one the other hand absorbing a phonon would create a photon of a frequency near cavity resonance, this process would be enhanced. So when we detune the laser to a side of the cavity resonance, we would enhance for instance upconversion, cooling the mirror, and reduce downconversion, heating it. In this way a net cooling of the mirror will occur.

To increase the amount of cooling (heating), we have to be sideband resolved:  $\kappa < \Omega_m$ . We now have the possibility to detune our laser to  $\omega_c \pm \Omega_m$ , with the result that we send a beam at the cavity that is outside of the cavity linewidth and thus cannot enter, expect by upor downconversion so that it is at the cavity resonance frequency. In this way we don't only enhance e.g. cooling versus heating, but almost completely suppress the opposing effect, see Fig. 4.1. This effect can in principle be used to cool the mirror to a phonon occupation number  $n_m < 1$ , which permits ground state cooling [7].

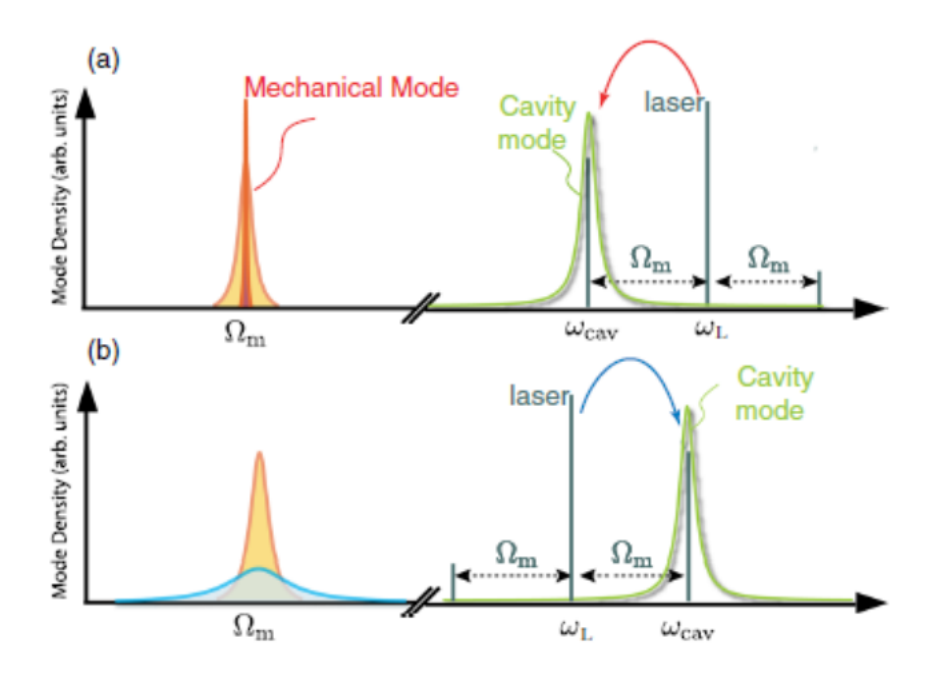


**Figure 4.1:** Schematic of cooling through Stokes scattering. If we detune the laser toward the right as in (a) only photons that deposit a quantum of energy can enter the cavity and the mirror is heated. In (b) the opposite effect is shown. The area of the density of states is proportional to the temperature of the oscillator. Original picture due to Aspelmeyer et al. [7].

#### 4.2 The Standard Quantum Limit

Back-action is the general term we apply to the effect of a measurement on the variable or system that we want to measure. We cannot, for instance, measure the position of a particle, using light, without altering, by the interaction between the particle and photon, the momentum of the particle, which in turn causes an uncertainty in the later position of the particle. In quantum mechanics this is usually explained by pointing out that certain observables don't commute, so that a change in one affects the other. When we then calculate their respective variances, we obtain a relation between the uncertainties in both observables, finding out that one can only shrink in proportion to the growth of the other.

Let's say we want to calculate an external force acting on our movable mirror, by measuring its position over time using light. However weak we choose our measurement beam, it will always exert a force on the mirror. And if this force is larger than the force that we are trying to measure we cannot with certainty say we measure anything but the effect of our own measurement beam on the mirror. Now, a part of the force exerted on the oscillator by our measurement beam is just a constant radiation pressure which shifts its equilibrium position. This can be accounted for: an external force would just cause a disturbance in the motion of the mirror around this new equilibrium. But since the emission of light by a laser occurs randomly in discrete packages, it suffers from shot noise. If N is the average number of photons that hit the mirror every moment, there will always be a  $N/\sqrt{N}$  signal to noise ratio that cannot be dealt with as we did with the constant pressure. Shot noise is inherently random. The fluctuations that arise from it will behave as white noise at all frequencies, including the mechanical resonance frequency. In this way they will effectively drive the mirrors motion. Since the signal to noise ratio is  $N/\sqrt{N}$  using a very weak laser beam means that the fluctuations will be relatively large. But increasing N will of course increase our signal to noise ratio at the cost of also increasing the absolute amount of noise  $\sqrt{N}$  generated this way.

We can distinguish two cases, illustrated in Fig. 4.2. We can use a very weak beam, in which case we exert only a small force due to shot noise on the mirror. But the relative fluctuations will be of considerable size and the amount of photons that falls on the photodetector we use for our measurement will fluctuate greatly. And this is the 'imprecision noise' of Fig. 4.2. A photodetector measures intensity, so all the information about the external force should be present in the changes in intensity of the light reaching the photodetector caused by the mirrors motion. When the measured intensity thus fluctuates more due to shot noise than because of the effect we want to measure, we cannot see it. But when we increase the power of the laser beam, we enter the 'back-action noise regime', where the intensity of the beam is relatively stable. The problem is now that the absolute fluctuations in the amount of photons reaching the mirror will cause back-action noise at the mechanical resonance frequency  $\Omega_m$ , driving the motion of the mirror. This additional driving can mask the effect of the external force, and only increases with increasing laser power.

The ideal point where one can measure is where both sources of noise are of equal size. This point is called the Standard Quantum Limit (SQL) of continuous position detection [7]. The method of back-action evasion is based on the desire to delve under this limit and measure more precise. We want to use a strong laser beam without paying the price of back-action forces on the mirror. To understand how we can do this, we must switch to another conceptual picture: that of Heisenberg's uncertainty relations.

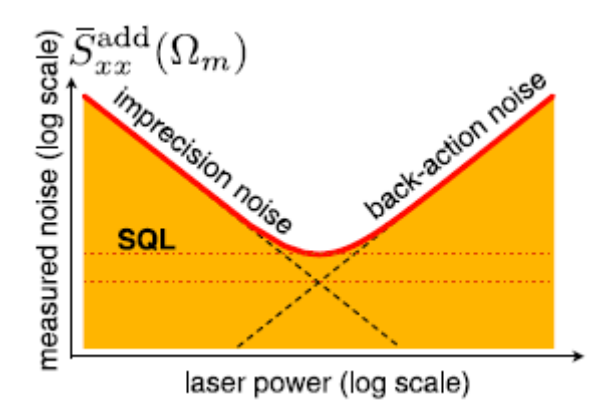


**Figure 4.2:** Contributions to the added noise (does not include e.g. thermal noise or the noise stemming from the measurement apparatus) from the imprecision caused by using too few photons and the back-action at increased laser power. Since we cannot evade imprecision noise, we use a high power laser and evade the back-action it causes. In this way we want to measure below the dashed red line of the SQL. Original picture due to Aspelmeyer et al. [7].

## 4.3 Back-Action Evasion: Heisenberg Picture

In order to understand how we can remove this back-action effect from our measured values, we have to see the problem from another angle. In the above I tried to account for the physical, causal relation between the measurement beam and the system to be measured. But when we look at the observable properties of the mirror in terms of the uncertainty principle we gain some insight in the properties that make a certain observable react or be immune to the measurement induced back-action.

Position and momentum are non-commuting observables, i.e.:

$$[\hat{x},\hat{p}]\neq 0$$

which means that after we have made a measurement on one of them, the possible outcome of the other has changed relative to what we would have found had we measured that one first. After calculating  $[\hat{x}, \hat{p}] = i\hbar$  we can rewrite this condition in terms of the uncertainty in the exact outcome of a measurement so that:

$$\Delta \hat{x} \Delta \hat{p} \ge \hbar/2 \tag{4.1}$$

This tells us that we can measure either the position or the momentum arbitrarily precise, yet at the cost of creating an equally large uncertainty in the other. And only when we measure once. One quickly faces problems when trying to measure the same system multiple times; let's say the position of a free particle at times spaced by an amount  $\tau$  in order to find out if an external force is present. We then find that the resulting uncertainty in the momentum leaks back into the position of the particle: because our measurement necessarily disturbed the particles momentum, its position after the measurement will be partly dependent on this change in momentum. So

$$\hat{x}(t_0 + \tau) = \hat{x}(t_0) + \hat{p}\tau/m \tag{4.2}$$

from which follows:

$$[\hat{x}(t_0), \hat{x}(t_0 + \tau)] = i\tau\hbar/m$$
 (4.3)

So if we measure some time  $\tau$  after our initial measurement, the disturbance will have increased proportionally. If this disturbance is greater than the effect we try to measure, it is essentially buried under this back-action noise. Yet this does suggest that if we measure fast enough, this disturbance will be kept to a minimum (as  $\tau \to 0$ ). But we will only shift the problem from the quantum mechanical uncertainty to the classical back action problem. Now the position may perfectly commute with itself, meaning that measuring does not add uncertainty, but at the cost of changing its actual course so much that we cannot measure any force smaller than the force exerted on the particle by the radiation pressure. For every measurement will change  $\hat{p}$ , which in turn changes  $\hat{x}$  via  $d\hat{x}/dt = \hat{p}$ . It follows from Eq. 4.2 that the course of  $\hat{x}$  will be disturbed more as  $d\hat{x}/dt = \hat{p}$  increases from its free evolution, making it harder to determine the effect of a possible external force. What we now measure is simply the effect of our own measurement. This reproduces the problem between using too few or too many photons. (A good way to think about it is to say that if we want to measure a gravitational wave with period P using a harmonic oscillator on which the wave will exert a force, measuring with period P/2 for instance will twice impart a certain momentum on the oscillator during the period that the gravitational wave exerts its influence. We can readily imagine that the effect of the wave becomes obscured by the random changes in momentum imparted by the measurement; the more often we measure the less clear is the signal from the wave [12]).

But we are not interested in a free particle, but, as in the example above, in a harmonic oscillator. Does it fare any better for its position and momentum? It certainly does not. Whereas one could at least in principle measure the momentum of a free particle without influencing its later position (the problem is that nobody knows an accurate method to do this [12]), in a harmonic oscillator you cannot measure either variable without disturbing, through the influence of the other, the variable you tried to measure. The momentum of an oscillator is as dependent on position as the other way around(which is not the case for a free particle). But as it turns out, we can also make use of the fact that it is an oscillator, as its position is a time dependent variable which oscillates sinusoidally and can be written as  $\hat{x}(t) = Acos(\omega t - \phi)$ , with A the amplitude,  $\phi$  the phase angle determining at what times the position reaches the max amplitude and  $\omega$  some angular frequency. Using basic trigonometry \*, we can write

$$\hat{x}(t) = \hat{X}_1 cos(\omega t) + \hat{X}_2 sin(\omega t)$$
(4.4)

with  $\hat{X}_1$  being  $Acos(\phi)$  and  $\hat{X}_2 = Asin(\phi)$ . We will refer to them as the quadratures of the mirror's motion, due to their 90 degree phase seperation. Writing  $\hat{p} = md\hat{x}/dt$ , we find that  $\hat{X}_1$  and  $\hat{X}_2$  correspond to the real and imaginary part of the oscillator's complex amplitude [1]:

$$\hat{x} + i\hat{p}/m\omega = (\hat{X}_1 + i\hat{X}_2)e^{-i\omega t}$$
(4.5)

which is analogous to the classical case in that they are constants of the oscillator's motion. So, as long as no external force acts on the mirror, they will not change [1]

$$\frac{d\hat{X}_j}{dt} = \frac{\partial \hat{X}_j}{\partial t} - \frac{i}{\hbar} [\hat{X}_j, \hat{H}_0] = 0 \tag{4.6}$$

Since from 4.5 it becomes clear that  $\hat{X}_1$  and  $\hat{X}_2$  are functions of both  $\hat{x}$  and  $\hat{p}$  we do not expect them to commute; this they indeed do not, so measuring one does disturbs the free

 $<sup>*\</sup>cos(x - y) = \cos x \cos y + \sin x \sin y$ 

evolution of the other. However, the added uncertainty does not leak back into the measured observable (they are conserved quantities of the mirror's motion), and we can easily calculate that:

$$[\hat{X}_1(t_0), \hat{X}_1(t_0 + \tau)] = 0 \tag{4.7}$$

It has been shown that  $\hat{X}_1$  and  $\hat{X}_2$  are conserved in the absence of interaction with the outside world; they are simply the quantum mechanical analogue of the classical complex amplitude, rotating as the oscillator moves [12]. We can see this clearly by looking at Eq. 4.5 where, as the position and momentum of the oscillator change, the complex amplitude remains constant, while rotating clockwise in the phase diagram [1]. We can picture a phase diagram of  $\hat{x}$  and  $\hat{p}/m\omega$  for a harmonic oscillator, see Fig. 4.3. As the oscillator moves, the point in the phase diagram describing the system moves in a circle, from its rest positions at maximum amplitude, swinging with a large momentum through its equilibrium, on towards its other maximum and so on. During all that time the complex amplitude of the system does not change:  $\hat{X}_1$  and  $\hat{X}_2$  remain constant. This means that the system point seen in the phase space of  $\hat{X}_1$  and  $\hat{X}_2$  does not move (as the whole space rotates along with the point as seen in the phase space of  $\hat{x}$  and  $\hat{p}/m\omega$ ), see Fig. 4.3.

Now, the system point for a quantum mechanical system is not actually a point, since that suggests that we know exactly where or how fast the particle is. In the  $\hat{x}$  and  $\hat{p}/m\omega$  space, it is a surface of minimum size

$$\pi \Delta \hat{x} \Delta \hat{p} / m\omega \ge \pi \hbar / 2m\omega \tag{4.8}$$

which is then a circle. Since  $[\hat{X}_1, \hat{X}_2] = i\hbar/m\omega$  [1], this circle has the exact same size in the phase space of  $\hat{X}_1$  and  $\hat{X}_2$ . When the phase spaces initially overlap, we see that the error circle describing the system moves in the first space, but stays put in the other, which rotates relative to the first with the same angular velocity  $\omega$  as the system.

What happens if we measure, say, the position of the oscillator? We can picture this as making the error circle smaller in the  $\hat{x}$ -direction, at the cost of increasing its width along the  $\hat{p}/m\omega$ -axis, for the size of the circle can never fall below  $\pi\hbar/2m\omega$  according to Eq. 4.8, making it an ellipse. The problem is that this ellipse moves as the oscillator moves, thus spreading the initial increased uncertainty in momentum back to the position (after t =  $\pi/2$ ) and then back to the momentum again, see Fig. 4.3. We learn from this that:

- 1. A measurement on a harmonic oscillator of either observable  $\hat{x}$  or  $\hat{p}$  influences the uncertainty about the other after a certain time.
- 2. If one performs measurement spaced by exactly either a half or a full period of the oscillator, one can measure one variable arbitrarily precise (because at those points the uncertainty will be back into the unmeasured observable).

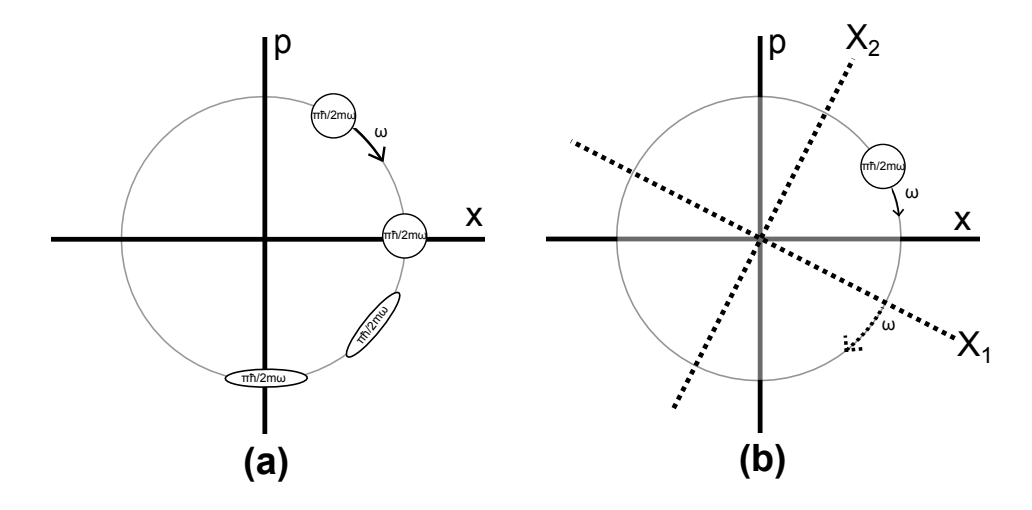


**Figure 4.3:** Left: position and momentum phase space of an harmonic oscillator, described by a system point rotating with angular frequency  $\omega$ . The system point has size  $\pi\hbar/2m\omega$ , reflecting the minimum uncertainty in both  $\hat{x}$  and  $\hat{p}$  when they are equally uncertain (then the system point is a circle) and after a measurement of position, at the cost of increased uncertainty in momentum (then system point is an ellipse). We see that at a later time, the uncertainty has traveled back to the position. Right: Quadrature (real and imaginary part of the complex amplitude) phase space of the same harmonic oscillator. Since the whole space rotates relative to the position-momentum space with angular frequency  $\omega$ , the system point does not move in it. A measurement made of one would result in an ellipse, which in principle can be made infinity thin. Original picture due to Caves et al. [1].

Thus position and momentum are, in the words of Braginsky  $et\ al.$ , 'stroboscopic quantum non-demolition observables' [1], and can be measured as accurately as one likes, given that one is satisfied with only two measurements per oscillation cycle. If one's measurements of the observable are optimal, the limit to how precise one measures is determined by the imperfection in the timing of the pulses  $\Delta t$  [1]. The reason it is called non-demolition is that measuring such an observable in a certain way does not alter the results of the next measurement in an unpredictable way. If we have made a first measurement, we can predict the outcome of the next one. This is what allows such measurements to measure a small external force, for if the measurement result differs from the expected value, we know we can attribute it to a external cause.

But if we imagine a measurement performed on  $\hat{X}_1$ , we find something that might even be better: since the system point does not move in the phase space of  $\hat{X}_1$  and  $\hat{X}_2$ , the increased error will remain in  $\hat{X}_2$ , no matter how often, and at what times, one measures  $\hat{X}_1$ . For these reasons we can call  $\hat{X}_1$  and  $\hat{X}_2$  continuous quantum non-demolition (QND) observables: measuring them continuously does not make them behave in an unpredictable manner. Of course, by measuring one we increase the uncertainty about the other significantly; but, as it does not leak back into the measured observable, we don't care.

In order to measure only e.g.  $\hat{X}_1$ , two methods are possible. Either we measure both  $\hat{x}$  and  $\hat{p}$ , so that we can make use of the identity

$$X_1 = \hat{x} \cos \omega t - (\hat{p}/m\omega) \sin \omega t \tag{4.9}$$

which follows from Eq. 4.5 and 4.4, making use of the annihilation and creation operators to express  $\hat{x}$  and  $\hat{p}$ . But we could also modulate our measurement in such a way that it depends

on  $\hat{x} \cos \omega t$ , making use of the fact that:

$$\hat{x} \cos \omega t = \hat{X}_1 \cos^2 \omega t + \hat{X}_2 \cos \omega t \sin \omega t \tag{4.10}$$

Using trigonometric identities we obtain:

$$\hat{x} \cos \omega t = \frac{1}{2} [\hat{X}_1 (1 + \cos 2\omega t) + \hat{X}_2 \sin 2\omega t]$$
 (4.11)

The beauty of which is that it depends only on  $\hat{X}_1$  if we average it in time, since the cosine and sine terms will average out to zero [12]. In the next section I will consider these options and show how we can use our system to perform a continuous measurement of  $\hat{X}_1$ .

4.4 The Hamiltonian 31

#### 4.4 The Hamiltonian

Given the analysis above, we need to devise a measurement scheme using the double trampoline resonator we have available. A recent paper by Clerk *et al.* addresses this issue, providing the complete quantum mechanical description of a measurement of a single quadrature of motion of a harmonic oscillator which is the back-mirror of a electromagnetically driven cavity [5]. In this section I will briefly discuss why they have chosen their method of measurement, and then explain how we can realize this with our system.

If we would be able to measure  $\hat{X}_1$  continuously, we have seen that the uncertainty generated by the measurement is all dumped into  $\hat{X}_2$ , and stays there: it does not leak back into  $\hat{X}_1$ . For this reason we call such a measurement back-action evading (BAE): the back-action of the measurement on the system we measure does not influence our subsequent measurements of the observable we are interested in. As discussed in the previous section, we could measure both  $\hat{x}$  and  $\hat{p}$  to obtain information about a quadrature of the motion, but then we need to have both a position and a momentum transducer; we could also perform stroboscopic measurements, which require a very precise timing. Or we modulate our measurement so that it depends on  $\hat{x}$  cos  $\omega t$ , so that we need only one transducer [12]. There exists a simple way to modulate our measurement sinusoidically, as described by Eq. (4.11) - by modulating the coupling strength between the single degree of freedom  $\hat{x}$  and a harmonic oscillator in a cavity [13]. Given also that continuous measurement can be more precise in theory than stroboscopic measurements [12] and that a momentum transducer of sufficient precision is difficult to realize [3], it makes sense that the authors of the paper our experiment is based on, have chosen the latter option of the three [5].

We need to obtain a coupling between the system that we want to measure and our detector. Ideally, the Hamiltonian describing this interaction is of the form [12]:

$$\hat{H}_I = K\hat{A}\hat{F} \tag{4.12}$$

with  $\hat{A}$  the observable we want to measure and  $\hat{F}$  the observable of the measurement apparatus we read out and K a constant describing the coupling between the oscillator and the measurement apparatus [1]. In the following section I will closely follow Aspelmeyer *et al.* [7] and present a derivation of the interaction Hamiltonian in the paper by Clerk *et al.* [5].

Given that we have a system consisting of a laser, entering a cavity, of which the backend mirror is an oscillator, the best way to realize a Hamiltonian of the form of Eq. (4.12)is to realize a coupling between the light in the cavity and the oscillator. Since the number of photons in the cavity  $\bar{n} = \langle \hat{a}^{\dagger} \hat{a} \rangle$  is dependent on the displacement of the mirror through G (see section 3.2) and can be measured with a photodetector, this will function as  $\hat{F}^{\dagger}$ . To arrive at the right coupling constant K we begin by writing down the Hamiltonian for the light in the cavity:

$$H_c = \hbar \omega_c \hat{a}^{\dagger} \hat{a} \tag{4.13}$$

It has as an expectation value simply the average amount of photons multiplied by their energy (of a single mode). But the cavity resonance frequency is coupled to the instantaneous displacement of the mirror:

$$\omega_c \to \omega_c(\hat{x})$$
 (4.14)

<sup>&</sup>lt;sup>†</sup>We see the movement of the mirror through the patterns in the amount of photons arriving at the photodetector after their interaction with the mirror.

We use a Taylor expansion then to obtain:

$$\omega_c(\hat{x}) \approx \omega_c + x \partial \omega_c / \partial x... \tag{4.15}$$

When we then assume that only the linear term suffices, as has been done in most theoretical work, without significant problems [7], and using the earlier obtained value for the coupling  $G = -\partial \omega_c / \partial x = \omega_c / L$  (see section 3.2 we obtain:

$$\hat{H}_c = \hbar \omega_c(\hat{x}) \hat{a}^{\dagger} \hat{a} = \hbar (\omega_c - G\hat{x}) \hat{a}^{\dagger} \hat{a}$$
(4.16)

Which consists of a part only dependent on the amount of photons and a part that deals with the interaction between the light and the mirror. Taking only that second part we obtain:

$$\hat{H}_{int} = -\hbar G \hat{x} \hat{a}^{\dagger} \hat{a} \tag{4.17}$$

But this is the Hamiltonian for measuring position, which is what we want to avoid. So, using equations (4.10) and (4.11) we multiply this Hamiltonian with  $\cos(\Omega_m t)$  and find:

$$\hat{H}_{int} = -\hbar G \frac{1}{2} [\hat{X}_1 (1 + \cos 2\Omega_m t) + \hat{X}_2 \sin 2\Omega_m t] \hat{a}^{\dagger} \hat{a}$$
 (4.18)

We can then discard the constant pressure which is the result of the photons in the cavity. This we do by splitting the cavity field  $\hat{a}$  in a constant average coherent amplitude  $\bar{a} = <\hat{a}>$  and a fluctuating term [7]:

$$\hat{a} = \bar{a} + \hat{d} \tag{4.19}$$

Making this substitution:

$$\hat{a}^{\dagger}\hat{a} = |\bar{a}|^2 + \bar{a}^{\dagger}\hat{d} + \bar{a}\hat{d}^{\dagger} + \hat{d}^{\dagger}\hat{d} \tag{4.20}$$

and discard that part of the Hamiltonian which is dependent on  $|\bar{a}|^2$ , being only caused by the constant pressure on the mirror. To do this, we need to displace the origin and then detune the laser accordingly [7] - this I have dealt with in section 3.2. If we have done so, we obtain an interaction Hamiltonian which deals specifically with the changes of the motion of the mirror relative to the shifted equilibrium position. Next we may assume that  $\bar{a} = \sqrt{n_c}$ ; we can make sense of this if we remember that  $|\bar{a}|^2$ , the square of the field in the cavity, is the amount of photons that make up the field [7]. The term dependent on  $\hat{a}^{\dagger}\hat{a}$  is so small that it does not factor in; thus, we can discard it [7]. But we should remember that unlike  $|\bar{a}|^2$  or  $\hat{a}^{\dagger}\hat{a}$ , the solitary annihilation and creation operators for the interaction Hamiltonian have an explicit time dependence as a consequence of the laser oscillations. The force experienced by the mirror changes as the phase of the incoming light changes, creating periodic fluctuations in the amount of photons hitting the mirror at certain times. Thus:

$$\hat{d} \to \hat{d}(t) = \hat{d}e^{i\omega_L t} \tag{4.21}$$

$$\hat{d}^{\dagger} \to \hat{d}^{\dagger}(t) = \hat{d}^{\dagger} e^{-i\omega_L t} \tag{4.22}$$

Performing the above calculations with this in mind, we are left with the following Hamiltonian:

 $\hat{H}_{int} = -\hbar G \frac{1}{2} \sqrt{n_c} [\hat{X}_1 (1 + \cos 2\Omega_m t) + \hat{X}_2 \sin 2\Omega_m t] (\hat{d}^{\dagger} e^{-i\omega_L t} + \hat{d} e^{i\omega_L t})$  (4.23)

32

4.4 The Hamiltonian 33

Which is perfect, for we now only need to use a low cutoff filter with  $\omega_{co} \ll \Omega_m$  (by averaging over a time  $\bar{\tau} \gg 2\pi/\Omega_m$ ), so that the oscillating terms in the Hamiltonian will average to zero over time, and we only select data about  $\hat{X}_1$  [3]. In this way we have created a Hamiltonian with  $K = -\bar{h}_1^1 G$ ,  $\hat{A} = \hat{X}_1$  and  $\hat{F} = \hat{d}^{\dagger} e^{-i\omega_L t} + \hat{d} e^{i\omega_L t}$ . It is the same equation that Clerk *et al.* [5] arrive at in their paper. The only difference is how they have defined  $\hat{X}_1$  and  $\hat{X}_2$ . They defined:

$$\Delta X_1 \Delta X_2 = \frac{1}{2} \tag{4.24}$$

So that Eq.(4.4) becomes:

$$\hat{x}(t) = x_{XPF}[\hat{X}_1 cos(\omega t) + \hat{X}_2 sin(\omega t)]$$
(4.25)

Whereas I have defined them, following [1]:

$$[\hat{X}_1, \hat{X}_2] = i\hbar/m\omega \tag{4.26}$$

So that:

$$\Delta X_1 \Delta X_2 = x_{zpf}^2 \tag{4.27}$$

With  $x_{zpf}$  the zero point fluctuations  $\sqrt{\frac{\hbar}{2m\Omega_m}}$  of the oscillator. The zero point fluctuations are enforced by the fact that the oscillator in its ground state would still have energy  $\hbar\Omega_m/2$ , causing a corresponding 'movement' or spread of coordinates around its equilibrium position. Both definitions occur in literature. I followed Caves *et al.* mainly for the sake of Fig. 4.3. It is a nice way to keep the area of the system point the same in both phase spaces.

#### 4.5 Back-Action Evasion: Wave Picture

We now know what kind of interaction the light field in the cavity and the oscillator causes back-action evasion, but when considering the practical conditions in which it works, it helps to write down what actually happens in the cavity in terms of electromagnetic waves interacting with each other. It will help to provide insight in how our periodic measurement allows us to evade the back-action associated with continuous measurement.

When performing a continuous measurement, one uses a laserbeam at the cavity's resonance frequency  $\omega_c$ . We however, want to modulate this beam with a wave of frequency  $\Omega_m$ . Starting with an electromagnetic wave of amplitude  $A_c$  en frequency  $\omega_c$  and modulating it with a wave of amplitude  $A_m$  and frequency  $\Omega_m$ :

$$A_c A_m e^{i\omega_c t} \cos(\Omega_m t) = A_c A_m e^{i\omega_c t} \left(\frac{e^{i\Omega_m t} + e^{-i\Omega_m t}}{2}\right)$$
(4.28)

Which we can also write as:

$$\frac{A_c + A_m}{2} \left( e^{i(\omega_c + \Omega_m)t} + e^{i(\omega_c - \Omega_m)t} \right) \tag{4.29}$$

We see that our original beam has been split into two beams (sidebands) spaced one mechanical resonance frequency above and below the original frequency. The condition for our scheme to work is that we are sideband resolved, meaning that these sidebands we've created cannot enter the cavity, as they are outside of the linewidth of the cavity ( $\kappa < \Omega_m$ ), see Fig. 4.4. The only way they can enter the cavity is by up- or downconversion as discussed in section 4.1, at which point they are again light at the cavity resonance frequency. But before they are scattered from the mirror they create an interference pattern in the cavity, which makes sure that all back-action noise at the mechanical resonance frequency is upconverted to noise at  $2\Omega_m$ , where it is no longer dangerous. But their own interference with light at the cavity resonance frequency also has components at  $\Omega_m$ , resulting in added noise. This is why they may not stay in the cavity 'on their own' and why it is so crucial to be sideband resolved: we cannot have sidebands in the cavity at the same time as light at the cavity resonance frequency and certainly not at the photodetector. I will discuss this in more detail in the next chapter.

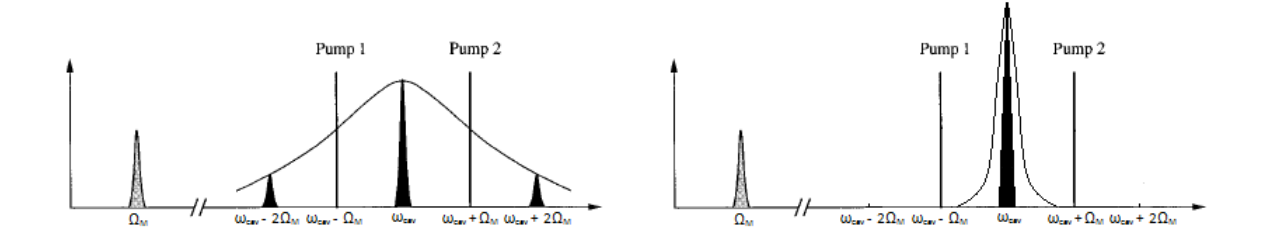


**Figure 4.4:** Using the two laser pump scheme in the case of a non-sideband resolved cavity, we see that in the left picture the sidebands can enter the cavity since they are within its linewidth, generating noise at the mechanical resonance frequency. However, in the right picture we see that when  $\Omega_m \gg \kappa$ , the sidebands are almost completely unoccupied. They only enter when they are upor downconverted to light at the cavity resonance frequency. Original picture is due to Bocko *et al.* [3].

In this section I will show how the sidebands remove unwanted back-action noise.

Let's assume we have a system consisting of the two sidebands of large amplitude *A*, and a noise term of very small amplitude *B*, which oscillates at the mechanical resonance frequency.

$$y(t) = A\sin(\omega_c + \Omega_m)t + A\sin(\omega_c - \Omega_m)t + B\sin\Omega_mt \tag{4.30}$$

We can calculate the amount of energy contained in this system by squaring it:

$$y^{2}(t) = A^{2}[\sin^{2}(\omega_{c} + \Omega_{m})t + \sin^{2}(\omega_{c} - \Omega_{m})t + 2\sin(\omega_{c} + \Omega_{m})t\sin(\omega_{c} - \Omega_{m})t]$$

$$+ AB[2\sin\Omega_{m}t\sin(\omega_{c} + \Omega_{m})t + 2\sin\Omega_{m}t\sin(\omega_{c} - \Omega_{m})t] + B^{2}\sin^{2}\Omega_{m}t$$
 (4.31)

We can then notice that all terms with amplitude  $A^2$  oscillate far from the mechanical resonance and keep the motion of the mirror constant, since they cool and heat the mirror simultaneously with the same amplitude. The  $B^2$  term does oscillate at resonance but since  $B \ll A$ , this term is negligible. The terms that could pose a problem are those with amplitude AB: through constructive interference the small disturbance  $B \sin \Omega_m t$  might now seriously interfere with the motion of the mirror. But, in this case, the problem is only apparent. Using the angle sum and difference trigonometric identities, we can write these terms:

$$AB[2\sin\Omega_m t \sin(\omega_c + \Omega_m)t + 2\sin\Omega_m t \sin(\omega_c - \Omega_m)t]$$

$$= 2AB[\sin\omega_c t \cos\Omega_m t \sin\Omega_m t + \cos\omega_c t \sin^2\Omega_m t + \sin\omega_c t \cos-\Omega_m t \sin\Omega_m t - \cos\omega_c t \sin^2\Omega_m t]$$
(4.32)

Which becomes:

$$2AB\left[\sin\Omega_{m}t\sin(\omega_{c}+\Omega_{m})t+\sin\Omega_{m}t\sin(\omega_{c}-\Omega_{m})t\right]$$

$$=4AB\sin\omega_{c}t\cos\Omega_{m}t\sin\Omega_{m}t$$

$$=2AB\sin\omega_{c}t\sin2\Omega_{m} \quad (4.33)$$

So, the dangerous  $\Omega_m$  terms have been shifted to  $2\Omega_m$  terms in the force exerted on the mirror. Since the mirror is no longer resonant with this force, its amplitude will not be significantly effected by it. It will average out to zero in the course of multiple periods of oscillation. Using the properties of the measuring beam and the cavity we make sure that all possible disturbances are neutralized by destructive interference. In this manner we can see why it is so important that we only have sidebands. If we perform the calculations above, introducing a term  $C \sin \omega_c t$ , we find that we not only end up with a  $2BC \sin \omega_c t \sin \Omega_m t$  term (which might be very small as long as  $C \ll A$ ), but also with an  $AC \sin^2 \omega_c t \cos \Omega_m$  term, which is due solely to the measurement beam.

## 4.6 Power Spectral Density and Noise

Clerk *et al*. give a complete description of the relevant noise for the above mentioned conditions. In this section I will summarize the most important conclusions of their paper, which we use as the basis for our experiment.

They first derive the power spectral density for both quadratures of the mirror's motion, which gives us the distribution of the frequency component that make up our signal. They assume that the spectrum is symmetrical and then consider only values around zero frequency, or  $\omega \ll \kappa$ , because they assume that a homodyne detection scheme is used. We don't do this, and expect to find signals at their respective frequencies in a FFT (Fast Fourier Transform).

As could be expected, the noise spectrum is dependent on the occupation grade of thermal photons  $n_{th}$  (the more phonons there are, the more noisy our measurement becomes as a result of their motion), the back action  $n_{bad}$  which is a result of the fact that as long we're not completely sideband resolved, the sidebands can still enter the cavity without up- or downconversion. The interference between the sidebands and the light at cavity resonance will generate a back-action force on the oscillator at the mechanical resonance frequency (this will be discussed in more detail in the analysis section.) The  $\hat{X}_2$  quadrature will in addition be heated by the back-action  $n_{BA}$  resulting from our measurement of  $\hat{X}_1$  [5]. All these effects are expressed as amounts of phonons absorbed by the mirror:

$$S_{X_1}(\omega) = \frac{\gamma_m/2}{\omega^2 + (\gamma_m/2)^2} [1 + 2(n_{th} + n_{bad})]$$
(4.34)

$$S_{X_2}(\omega) = \frac{\gamma_m/2}{\omega^2 + (\gamma_m/2)^2} [1 + 2(n_{th} + n_{bad} + n_{BA})]$$
 (4.35)

with  $\gamma_m$  the damping rate of the mirror. The thermal occupation is given by the familiar expression:

$$n_{th} = \frac{1}{e^{\frac{\hbar\Omega_m}{k_BT}} - 1} \tag{4.36}$$

which can in principle be reduced by cooling the mirror before measuring. The back-action induced on the  $\hat{X}_2$  component is the result of our precision of measurement of  $\hat{X}_1$ , which is dependent on the coupling strength, the lifetime of photons in the cavity, the number of photons in the cavity and the fluctuations arising from the intrinsic damping (on a timescale  $1/\gamma_m$ ). The back-action on  $\hat{X}_2$  will be the inverse of our precision in  $\hat{X}_1$  and becomes  $\hat{X}_2$ :

$$n_{BA} = \frac{2G^2\bar{n}_c}{\kappa\gamma_m} \tag{4.37}$$

And finally, the back-action force on both quadratures, which disappears as one becomes 'more sideband resolved', limiting scattering to the sidebands at  $\pm 2\Omega_m$  (or higher).

$$n_{bad} = \frac{n_{BA}}{32} \left(\frac{\kappa}{\Omega_m}\right)^2 \tag{4.38}$$

<sup>&</sup>lt;sup>‡</sup>From Eq. **??** we can calculate the precision in  $\hat{x}$  (and from there to  $\hat{X}_1$  according to Eq. 4.4), making the assumption that the precision in the phase readout  $\partial\theta$  is proportional to  $1/\sqrt{n_c}$ . For a more complete discussion, see Aspelmeyer *et al.* [7]

<sup>§</sup>In Clerk *et al.* this equation is expressed differently, because they have chosen to define the quadratures differently. If we assume A = G and use their definition as in Eq. (4.25), we see that  $g = Gx_{zpf}\sqrt{n} = Ax_{zpf}\bar{a}_{max}$ , with g the optomechanical coupling strength [7].

When we measure, the light intensity reaching the photodetector will be transformed into a current, the power spectral density of which will be given by a gaincoefficient proportional to the local oscillator amplitude [5], the power density of  $\hat{X}_1$  and additional noise arising from the cavity drive and the detection itself. This added term can be split in a part consisting of actual noise, multiplied by of the limitation imposed by shot noise (see section 4.2).

$$S_I(\omega) = Q^2 \left[ S_{X_1}(\omega) + S_0 \frac{\kappa}{8G\bar{n}_c} \right]$$
 (4.39)

with Q the gain coefficient and  $S_0$  the actual noise in arising from the detector and drive, in such a way that if we are only limited by shot noise,  $S_0 = 1$  [5]. It can immediately be seen that the second term is dependent on the amount of photons in the cavity; increasing the laser power reduces it thus greatly (amount of photons being the square of the amplitude of the field). The problem is that doing this increases  $n_{bad}$  accordingly. Clerk  $et\ al$ . define this condition more clearly and give a limit we must reach to beat the SQL (total added noise  $n_{add} < 1/2$ )  $\P$ . Since the total added noise can be written as:

$$n_{add} = n_{bad} + \frac{\kappa \gamma_m}{32G^2 \bar{n}_c} = \frac{n_{BA}}{32} \left(\frac{\kappa}{\Omega_m}\right)^2 + \frac{1}{16n_{BA}} S_0$$
 (4.40)

which follows from the previous equations if we have reasoned back to the noise in the cavity by dividing Eq. (4.39) by  $Q^2$  and looking at the case where  $\omega=0$ , i.e. when we are at resonance  $(S_{X_1}(0))^{\parallel}$  [5]. In the case that  $\kappa/\Omega_m \to 0$ , we see that if  $n_{BA} \geq 1/8$ , then  $n_{add} < 1/2$  and we've beaten the SQL. And in the case of a finite  $\kappa/\Omega_m$  we find that at the value:

$$n_{bad} = \frac{\Omega_m}{\kappa} \sqrt{2S_0} \tag{4.41}$$

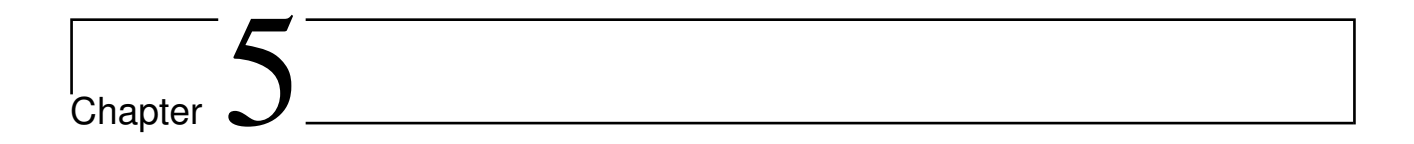
we have a minimum of:

$$n_{add} = \frac{\kappa}{8\Omega_m} \sqrt{\frac{S_0}{2}} \tag{4.42}$$

which beats the SQL for experimentally feasible values [5]. In our case  $\frac{\kappa}{\Omega_m} \approx 0.07$  (see section 3.3) if all is optimal, but using a lower grade sample for instance a finesse of 20000 would suffice to make  $\frac{\kappa}{\Omega_m} \approx 0.6$ , so we need to achieve  $S_0 \leq 100$  to stay under the SQL.

 $<sup>\</sup>P$ A way to understand why the standard quantum limit is half a phonon is to think of the Hamiltonian of a harmonic oscillator in its ground state:  $\frac{\hbar\Omega_m}{2}$ , which is half a phonon of energy. The resulting movement, or spread of coordinates in the groundstate is what enforces the uncertainty of the zero point fluctuations. But we can also regard this value as stemming purely from our measurement. In that case it is found that the SQL for continuous position detection is the combined effect of the imprecision noise and the back-action noise at their optimal values (when they are equal, see Fig. 4.2), both adding  $\frac{\hbar\Omega_m}{4}$ . But then we find that only the back-action actually heats the oscillator, whereas the imprecision noise is just of the same magnitude as thermal noise of  $\frac{\hbar\Omega_m}{4}$  [7].

Clerk *et al.* assume homodyning, which is a process wherein one mixes the measured signal with a local oscillator of the same frequency. If both are at  $\omega_c$  then the eventual result after mixing will have the information around  $\omega_c$  around  $\omega=0$ .



### 5.1 Finesse

To measure the finesse (and therefore  $\kappa$  ) of a cavity, you want to send in a short pulse of light at the resonance frequency, and measure the exponential decay of the amount of light that exits the cavity. The pulse we created with an AOM. If we turn off the sound wave traveling through the crystal, the first order beam will vanish. Since the AOM has a very quick response time, we can create pulses of light by switching the first order beam on and off. The problem is however that the laser - the Toptica - is performing a sweep\* so that just sending in block waves will not have the desired effect of pulsing the light at resonance, as we have no control over when the AOM shuts off compared to the frequency of the sweep. Therefore we must connect the oscilloscope to the AOM driver so that it only shuts off when a certain intensity of transmission is measured, and then stays off long enough for the cavity to decay without interference.

In this way we can measure the exponential decay time  $\tau_c$ , but how is this connected to the finesse and  $\kappa$ ? We have to think back to what happens in a cavity when light is either reflected or transmitted by it. Small phase changes build up destructive interference in the cavity for light of a wavelength not resonant with the cavity, but create a standing wave when the light is resonant with it. The more reflective the mirrors, the longer light would be trapped in the cavity; this would result in more phase changes building up to destructive interference. So the reflectivity of the mirrors determines how much off resonance light can be and still enter the cavity, because the more reflective they are, the smaller the phase change 'per bounce' that still adds up to destructive interference. Also, the other way around: the more reflective the mirrors, the larger the amplitude of the standing wave of resonant light. Now all the elements are conceptually present: the decay time tells us the reflectivity of the mirrors and the reflectivity can be used to calculate the linewidth of the cavity (and thus the finesse).

$$\tau_c = \frac{n}{c} \frac{L}{1 - R} \tag{5.1}$$

The decay time  $\tau_c$  can be calculated by taking the time light takes to travel the length L of the cavity once, which is simply the length divided by the speed of light c in a certain

<sup>\*</sup>There are two ways of making sure that light gets into the cavity: sweeping and locking. To sweep means to let the laser periodically change its frequency around some center frequency, so that - if you sweep across a free spectral range - you will certainly be at cavity resonance twice every sweep. These sweeps are usually performed at around 10 Hz, meaning that we sweep 10 free spectral ranges every second. This determines the time the laser light can enter the cavity. One can also lock the laser to the cavity, as I have explained in 3.6, so that the light always enters the cavity.

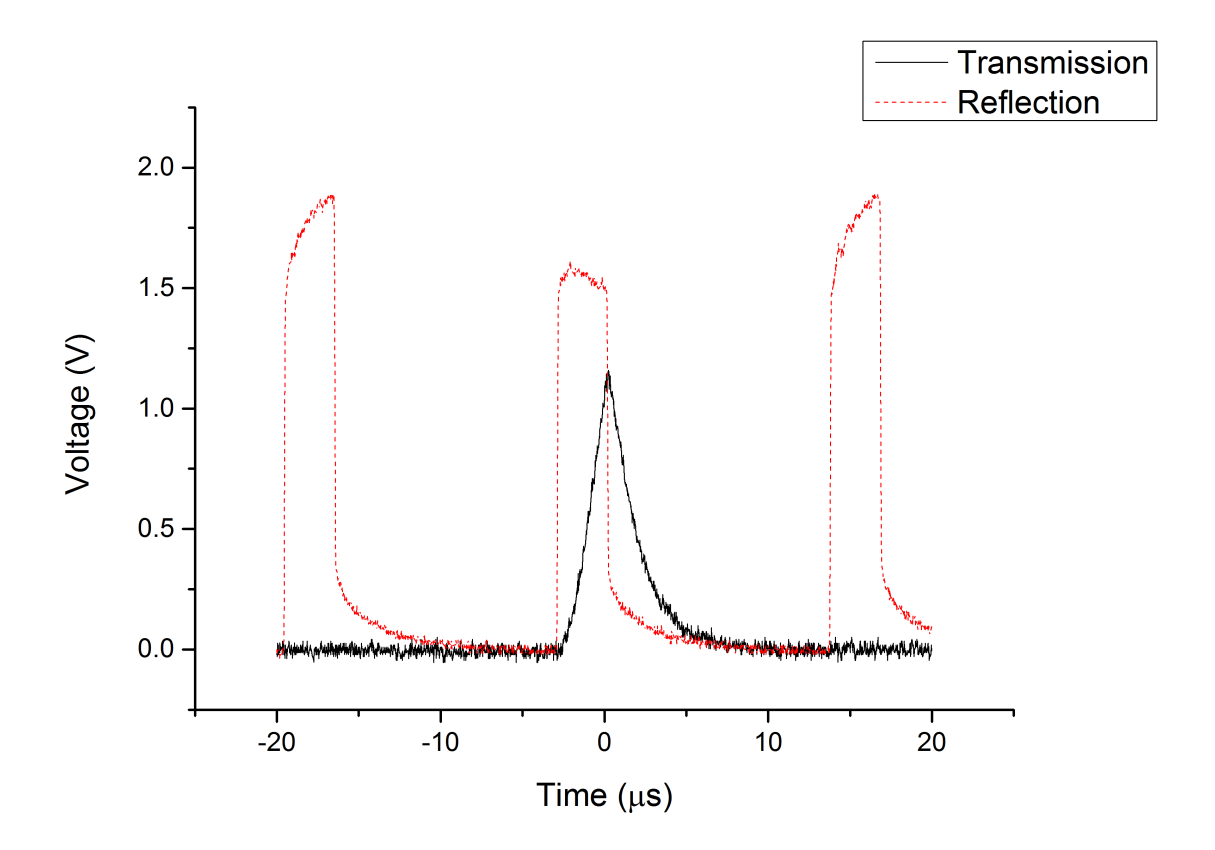


**Figure 5.1:** Reflection and transmission signal from the cavity measured with photodetectors. We see that the reflected light is pulsed in such a way that it falls to zero while the cavity is still being filled light is being transmitted through the first mirror, so that we can measure the decay time of the light leaving the cavity.

material with refractive index n (in our case n = 1). This number must then be divided by the transmission coefficient 1 - R, with R the reflection coefficient of the mirrors. If R = 0, then all light is transmitted and  $\tau_c$  is equal to the time it takes light to travel once between the two mirrors. However, as R increases, so does  $\tau_c$ , the average time a photon remains in the cavity. The finesse can then be calculated as a function of R:

$$F = \pi \frac{\sqrt{R}}{1 - R} \tag{5.2}$$

For a nice derivation of this result see [14].

For the measurements we actually performed, we made images with an oscilloscope like Fig. 5.1 of the transmission signal and used an exponential decay fit in Origin on the slope after the AOM had shut off. This gave us the exponential decay time. Using Eq. (5.1), with  $L = 5 * 10^{-2} \pm 0.1 * 10^{-2}$ m and  $c = 2.998 * 10^{8}$ m/s, we can calculate  $R^{+}$ . From this we've calculated the finesse using Eq. (5.2). The estimated error in  $\tau_c$  is the fitting error calculated by Origin. I've always used a forced fit, fixing the starting point of the decay:  $x_0$ . Since we did not exactly measure the cavity length, the finesse can only be approximated.

In Table 5.1 we see the decay times for four different measurements. Mirror 7 was the first mirror we used - one sample contains 16 mirrors. It was larger than mirror 4 and there-

<sup>&</sup>lt;sup>†</sup>These finesse measurements are all done once, without accurate data about the actual length of the cavity. To distinguish different calculated reflectivities we need at least four relevant digits. For this reason I've not included them in . To give an idea however, for a finesse of 20000, the reflectivity would be  $\approx 0.9998$ .

5.1 Finesse 41

**Table 5.1:** Table of the measured exponential decay time of the two mirrors we used. For mirror 4 several measurements have been included. The finesse and the linewidth  $\kappa$  have been calculated according to Eq. (5.1), Eq. (5.2) and Eq. (3.2). Included is also how sideband resolved the system with these parameters is. Note that mirror 7 had another resonance frequency than mirror 4. ( $\approx$  120 and  $\approx$  320kHz respectively.)

	$ au_c$	F	$\kappa$	$\frac{\Omega_m}{\kappa}$
Mirror 7	$1.817 \pm 0.013 \mu s$	$\approx 34000$	$\approx 2\pi * 88000$	$\approx 1.36$
Mirror 4(1)	$0.905 \pm 0.028 \mu s$	$\approx 17000$	$\approx 2\pi * 175000$	$\approx 1.82$
Mirror 4(2)	$1.072 \pm 0.012 \mu s$	$\approx 20000$	$\approx 2\pi * 150000$	$\approx 2.13$
Mirror 4 Vacuum	$0.790 \pm 0.007 \mu s$	$\approx 15000$	$\approx 2\pi * 200000$	$\approx 1.6$

fore easier to align. We see that the reached finesse ( $\approx 34000$ ) is also higher. Yet we would have expected, based on measurements once performed on this mirror to have reached at least 50000. That we did not reach this can have multiple causes, but I will mention the most important two. The sample was old, and may have been damaged or dust may have gotten on it. The quality of the mirrors will be affected by these things. And we had to align by hand. We did not use piezo motors to align our cavity, and all the precision work had to be done by hand. This could hinder our ultimate precision and thus the finesse we can reach.

Mirror 7 had a linewidth of  $\kappa = \frac{c}{2FL} \approx 2\pi * 88 \text{kHz}$ . We found that its mechanical resonance frequency was  $\approx 2\pi * 120 \text{kHz}$ , and decided that this was not sideband resolved enough. We aimed for at least  $\frac{\Omega_m}{\kappa} = 2$ , so we were not satisfied with the  $\frac{\Omega_m}{\kappa} \approx 1.36$  we got. So we aligned on another mirror (number 4). I've included one unsatisfactory measurement in Table 5.1(Mirror 4(1)) and the one we eventually decided was the best we could reach (Mirror 4(2)). The finesse is clearly lower than that of mirror 7, yet being a lot smaller, its mechanical resonance frequency turned out to be  $\approx 2\pi * 320 \text{kHz}$ . With  $\kappa \approx 2\pi * 150 \text{kHz}$ , this would mean that  $\frac{\Omega_m}{\kappa} \approx 2.13$ . But when we hung the optical bench in the vacuum chamber the signal would disappear and we had to realign. With the bench hanging vertically and loosely, this proved to be so difficult that we could only reach a finesse (Mirror 4 Vacuum) of  $\approx 15000$ , giving a  $\kappa \approx 2\pi * 200 \text{kHz}$  and  $\frac{\Omega_m}{\kappa} \approx 1.6$ . So we had improved, but not by much. Because of the time scheduled for my Bachelor research we decided to move forward anyhow, since we reasoned that we could at least perform classical BAE measurements, given that Clerk et al. for  $\frac{\Omega_m}{\kappa} = 2$  already predict that one is able to delve below the SQL [5].

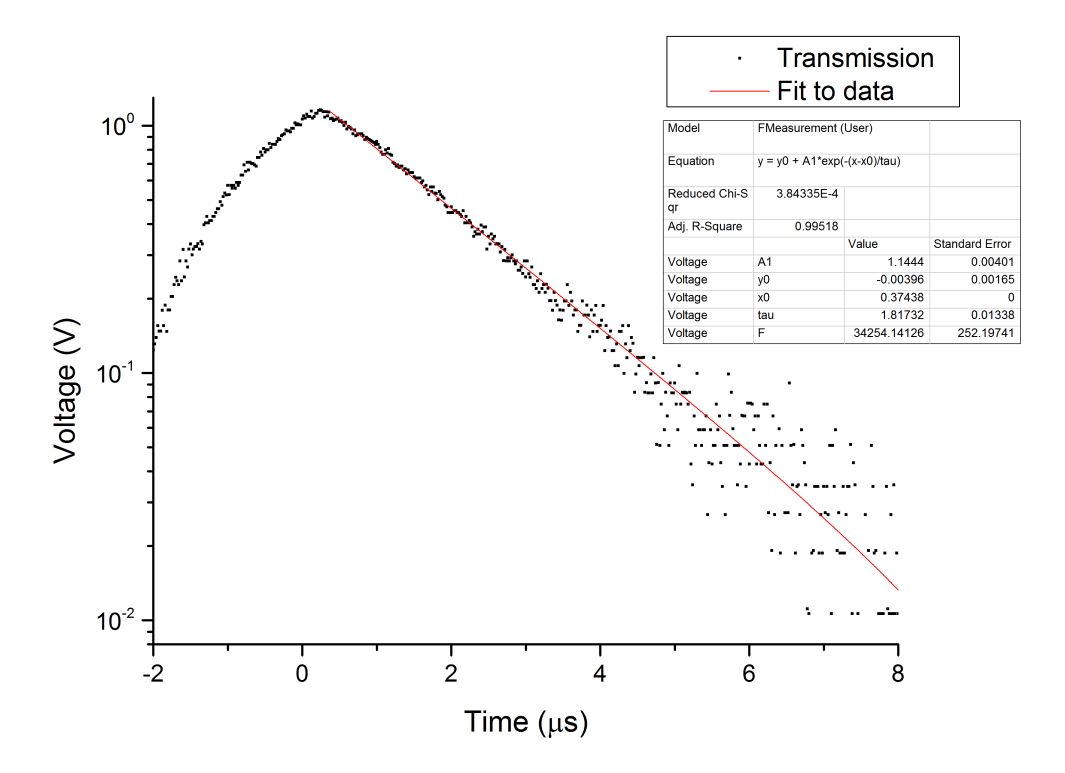


**Figure 5.2:** Oscilloscope measurement of the transmitted light. When the AOM shuts off, the amount of light transmitted starts to decay. This is mirror 7 and the highest finesse that we have measured. The figure also shows the Origin fitting data.

## 5.2 Quality

We also needed to find out what the resonance frequency of our oscillator was. Our sample consisted of a chip, wherein sixteen small mirror had been etched out (for details about the fabrication process see Ref. [6]). These mirrors have different sizes and qualities and some are faulty, so we had to first find one that could in principle work and then check whether we could build a good cavity with it. Only after those steps could we determine its resonance frequency. The intuitive trade-off we had to make was between a smaller mirror having a higher resonance frequency, but which would be difficult to align; and a larger mirror having the opposite qualities. After a failed first round <sup>‡</sup>, we settled on the smallest mirror we could find.

To determine the resonance frequency we locked the laser to the cavity at the resonance frequency and made a FFT of the signal coming from light falling on the photodetector. The result shown in Fig. 5.3 is obtained with a PDH lock using light falling on the reflection detector. We found a mechanical resonance frequency  $\Omega_m$  of  $\approx 2\pi * 321$ kHz.

From this fit we can obtain the FWHM of the peak, which gives us the linewidth of the oscillator  $(\gamma_m)$  which we can use to calculate its quality factor Q. The linewidth is a measure for the dissipation rate of energy stored in the oscillator. Its relation to the quality factor is:

$$Q = \Omega_m / \gamma_m \tag{5.3}$$

The quality factor is then a measurement for the degree of decoupling from the other

<sup>&</sup>lt;sup>‡</sup>We reached a finesse of around 30000, which meant that our cavity linewidth was  $\omega_{fsr}/3*10^4 \approx 2\pi*10*10^5$ . We thought this initially fine, but the resonance frequency turned out to be around 120kHz, making us hardly sideband resolved.

5.2 Quality 43

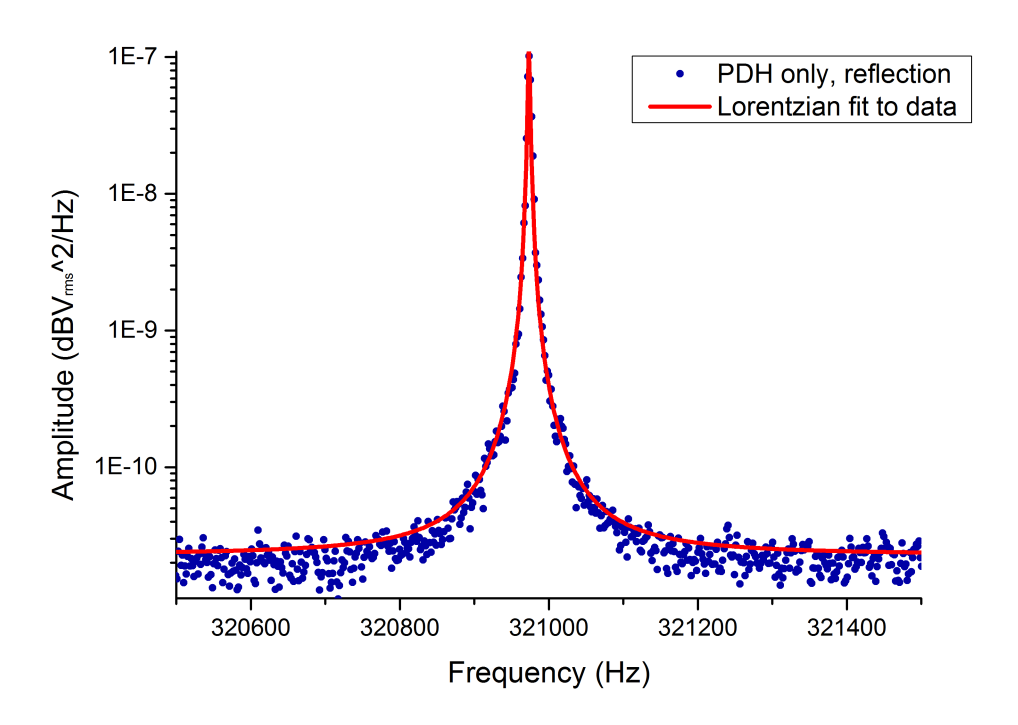


Figure 5.3: Lorentzian fit to FFT of reflection signal using only a weak laser PDH locked to resonance.

modes [1].

A measurement as shown in Fig. 5.3 can be used to determine the temperature of the mirror if we cool or heat it, following Aspelmeyer *et al.* [7]. For the noise power spectral density which the FFT measures is related to the variance in the mechanical displacement via:

$$\int_{-\infty}^{\infty} S_{xx}(\omega) \frac{d\omega}{2\pi} = \langle x^2 \rangle \tag{5.4}$$

with  $S_{xx}(\omega)$  the power spectral density of the oscillator and  $\omega$  some frequency. Using then the equipartition theorem:

$$\langle x^2 \rangle = k_B T / m_{eff} \Omega_m \tag{5.5}$$

with  $k_B$  Boltzmann's constant, T the temperature of the oscillator and  $m_{eff}$  the effective mass of the oscillator. The problem however, is that when we perform an FFT we do not immediately get the right dimensions on the y-axis. In our case they are expressed in  $V_{rms}^2/Hz$  since it is a measurement of the voltage in a photodetector and not of the light or the oscillator directly. So we need a gauge to determine how the response of our photodetector is related to the actual noise spectrum of the oscillator. To do this one should measure at the cavity resonance frequency, neither cooling nor heating, so that the temperature of the mirror is known beforehand to be room temperature (293K). We can then calculate the conversion rate between the area measured (in  $V_{rms}^2/Hz$ ) and  $< x^2 >$  which is expressed as  $m^2/Hz$ . In this case, taking for the mass  $\approx 100$ ng [15], we find that we need to multiply our found area of  $\approx 7.11*10^{-7}$  with  $\approx 2.8*10^{-14}$  to obtain the power spectral density in terms of the mirror's displacement.

If we perform such gauge measurements on the transmission detector when the measurement beams and PDH are turned on, we can quantify the effect of our BAE evasion scheme

in terms of heating of the oscillator. When we inject noise at the mechanical resonance frequency in the cavity we expect the oscillator to be heated accordingly. We then can measure the oscillator's temperature as a function of the position of the sidebands and show that when they are positioned at  $\omega_c \pm \Omega_m$ , we remove the back-action of the noise on the mirror and its temperature will not increase or increase less relative to when no noise was present. See section 4.1 for a detailed explanation of cooling and heating, section 4.5 for an explanation of why our BAE scheme removes noise at the mechanical resonance frequency and section 5.4 for the noise that we inject.

### 5.3 Amplitude Modulation

In order to create the sidebands necessary for our BAE scheme, we need to modulate our original beam in the aforementioned way:

$$\sin(\omega_c t)\sin(\Omega_m t) = \sin(\omega_c + \Omega_m) + \sin(\omega_c - \Omega_m)$$
(5.6)

This is a form of amplitude modulation called double sideband suppressed carrier amplitude modulation (DSB-SC modulation). In this chapter I will sketch the principles of amplitude modulation and show that our system is capable of performing the right kind of modulation.

The basic idea of standard amplitude modulation is that a high frequency electromagnetic wave (the carrier) is varied in amplitude according to the form of some lower frequency wave (the modulation).

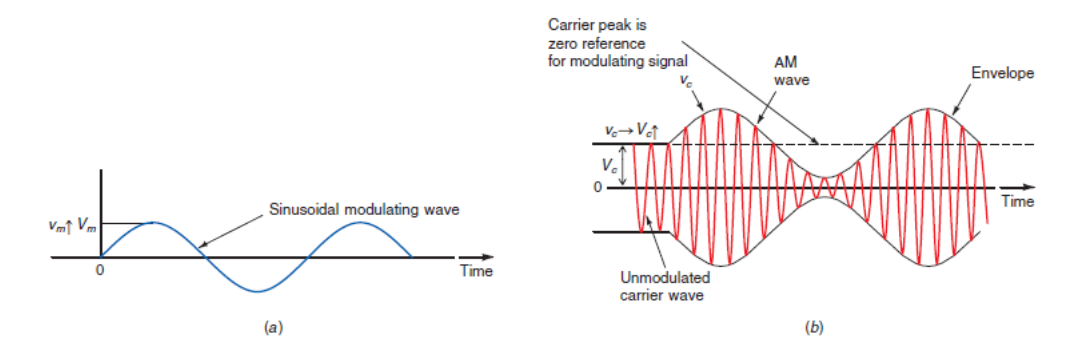


**Figure 5.4:** Left: the modulating signal. Right: the carrier wave is being modulated so that it will vary in amplitude at the frequency of the modulating signal. Picture taken from [16].

So if we have a carrier wave of amplitude 1 and we modulate it with a modulation wave of amplitude 0.5 (both waves are continuous sine waves), the resulting beam will oscillate not only between 1 and -1 due to its original amplitude, but it will periodically vary between oscillations between 1.5 and -1.5 and between 0.5 and -0.5. To put it into formula, a carrier wave of amplitude  $V_c$  and frequency  $f_c$  will have an instantaneous value  $v_c$  of:

$$v_c = V_c \sin(2\pi f_c t)$$

And a modulation wave of amplitude  $V_m$  and frequency  $f_m$  will have an instantaneous value  $v_m$  of:

$$v_m = V_m \sin(2\pi f_m t)$$

So that the resulting wave will look like this, taking into account that the original beam is modulated to increase and decrease in proportion to the modulating frequency around its original amplitude (therefore the extra '1', signifying the presence of carrier):

$$v_r = (1 + V_m \sin(2\pi f_m t)) V_c \sin(2\pi f_c t) = V_c \sin(2\pi f_c t) + V_c V_m \sin(2\pi f_m t) \sin(2\pi f_c t)$$
 (5.7)

We clearly see that it is the second term which we are interested in (compare to 5.6). But one cannot select this term by, for instance, increasing the modulation amplitude so that the second term would become much larger than the unwanted carrier; this is called overmodulation. In some systems this cannot be done principally, for you are effectively modulating the output *power* of your wave; the power of course cannot go below zero, so

that a modulation larger than the original beam would result in a 'clipping' of the beam, which creates a distorted waveform, a sine wave of which the negative peaks have been cut off. The condition that needs to be fulfilled to create DSB-SC modulation is that the carrier can undergo a phase shift when the modulating beam becomes larger than the carrier. In systems in which this occurs we expect the output power to oscillate at twice the modulation frequency, as it increases again where it previously was still falling. But to do this correctly still means to either increase the modulation to a point where we can neglect the carrier or to find a system which does not transmit the carrier at all. If we cannot increase the modulation enough we expect to see in the first case an output (power)signal with peaks of different sizes, with the small peak increasing as the modulation strength is increased. This follows from Eq. (5.7). For instance, if A = 1 and B = 3 we will see a large peak oscillating between 4 and -4 and a small peak between 2 and -2, which has undergone a phase reversal, during every period of the modulating waveform. DSB-SC however, would look like a regular sine wave, just oscillating at twice  $f_m$  - this follows from Eq. (5.6).

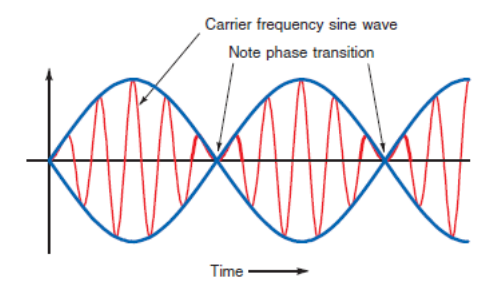


**Figure 5.5:** Schematic drawing of DSB-SC modulation. Notice the phase shift every half period of the modulation. This follows quickly from Eq.5.6. Picture taken from [16]

We then faced the problem mentioned in the section on the wave picture of BAE. We needed to create sidebands at a mechanical resonance frequency away from the original beam, and wanted to do this by amplitude modulating the original beam. I also mentioned radio technology, where this is a common technique. What I didn't to mention was that it is very uncommon to perform a full modulation. It is quite a different story whether I want to let the amplitude oscillate a bit, or to fully turn it sinusoidally on and off at  $\approx 300 \rm kHz$ . A chopper for instance, would create a block-wave modulation, and reaches at most around 100kHz. A more elaborate scheme, using a beam splitter and the destructive and constructive interference of two beams, where one is sinusoidally phase shifted from 0 to 180 degrees relative to the other, was also not viable. We would need a very good phase shifter to do this cleanly at 300kHz, and these weren't lying around. So we turned to the AOM again.

We know that an AOM can be used to pulse light, by switching the first order diffraction beam on and off. The response time of the AOM is in the nanosecond range, well beneath the time we need to perform a 300kHz oscillation. The only problem with the AOM was that it also frequency shifted the beam, and our measurement scheme does not allow for this: we want to use one laser to perform both PDH and measurement. For this to work, both the measurement beam and the PDH beam need to be at the same initial frequency (we will of course turn the measurement beam into sidebands), otherwise the laser is stabilized to 80MHz off resonance, which defeats the purpose. To adjust for this inconvenience, we realized that using two AOM's we can return the beam to its original frequency, while still allowing us to amplitude modulate it around that frequency to create the sidebands. This required of course some re-aligning of the initial path, but it did not give us too much trouble.

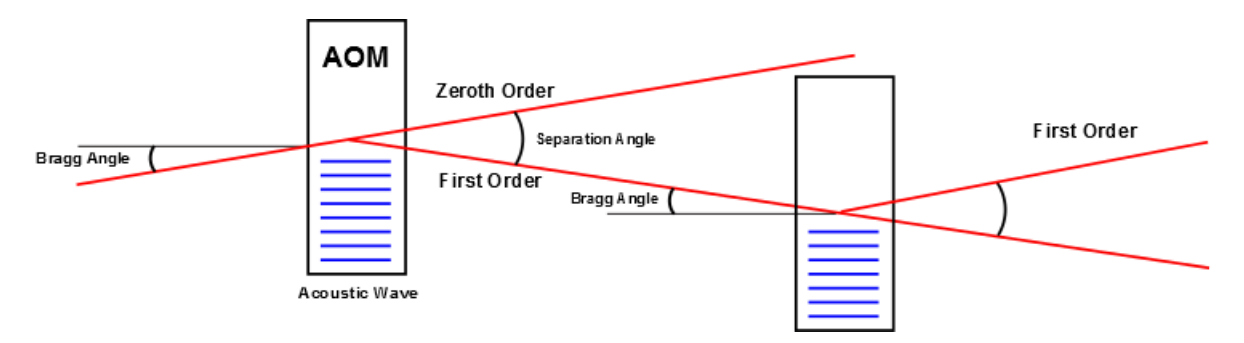


**Figure 5.6:** the beam is diffracted into the first order (m=-1), which is used as the incoming beam for the second AOM, where we again select the first, yet opposite, order of diffraction (m=1). The beam has now been frequency shifted twice, with the same frequency in opposite directions.

So knowing what we had to look for, we modulated the sound waves of our AOM, so that the first order diffracted beam would be modulated accordingly. We then looked at the light coming out of the AOM with a photodetector and experimented with the modulation settings. As it turned out, we were able to distinguish different kinds of modulation: regular modulation with the carrier also transmitted; overmodulation with increasing sizes for the small peak, and DSB-SC modulation. As long as we did not add any offset to our modulating signal, we would perform DSB-SC modulation automatically.

Looking at the left part Fig. 5.7 we see in the left picture an oscilloscope image of the light coming out of the AOM when the AOM is modulated with an 200mV offset along with a peak to peak voltage. The black line at 200mVpp oscillates at the modulation frequency  $f_m$ . If we increase the peak to peak voltage we see that instead of a regular sine wave, an extra peak develops in the valleys of the original signal. The red line (400 mVpp) shows only a flattening, but once we increase the voltage to 600mVpp an extra peak develops. This is perfectly in line with overmodulation according to Eq. (5.7). The phase shifts once every period of oscillation to develop into a small peak if the modulating amplitude becomes larger than that of the carrier. If we continue to increase the voltage, at some point the extra peak will still increase but the main peak will start to decrease, see the left picture of Fig. 5.8. It appears that the driving voltage is too high for the AOM and it can no longer produce a normal output. We can see this clearly in the left picture of Fig. 5.9, when both peaks are clipped and become increasingly smaller as the driving voltage increases. So we can distinguish these three regimes: in the left picture of Fig. 5.7 we see a modulated signal becoming overmodulated; in the left picture of Fig. 5.8 we see an overmodulated signal becoming more overmodulated until it is almost a  $2f_m$  signal; but in the left picture of Fig. 5.9 we see that we cannot drive it any higher because the waveform becomes distorted.

So, after seeing this, it made good sense that if we did not provide an offset to the AOM we would perform the right kind of modulation. We already witnessed the phase reversal during overmodulation. So looking at the right picture of Fig. 5.7, we indeed see a signal at  $2f_m$  (compare with the left picture: same timescale) that grows as we increase our modulation voltage. When we increase the voltage like we see in the right picture of Fig. 5.8, the point where we overdrive the AOM is much better defined, since the signal does not change significantly until we increase the modulation from 1.4Vpp to 1.6Vpp. This seems to suggest that once we modulate at 1Vpp we have already reached to point where light is maximally diffracted into the first order. Any further increase only provides more distortion, certainly

above 1.4Vpp. The right picture of Fig. 5.9 finally shows us the distorted signal, decreasing as the voltage is increased.

The only question that we still needed to answer concerned the amount of modulation that would provide the best result. 'The best' in our case would be an optimum between the amount of light diffracted into the first order and the purity of the sinewave (and thus our sidebands). As is clear from figures 5.8 and 5.9, above a certain modulation strength the AOM would no longer behave correctly, so that needed to be avoided. On the other hand, a modulation that is too weak might not completely suppress the carrier. The method that we used to find the right amount was to measure the relative strength of the Fourier components of the output signal at  $f_m$ ,  $2f_m$  and  $3f_m$  and in that way determine at what strength the beam would be purest.

Looking at Fig. 5.10 we see the  $f_m$  fourier component of the light emitted from the AOM divided by the  $2f_m$  component. All higher order components were so small that we did not include them here. Since we are looking for a pure sine wave oscillating at  $2f_m$ , it makes sense to say that at approximately 1Vpp we have the best signal. This fits nicely with the results of Fig. 5.8 and Fig. 5.9, where we see that at 1Vpp the light is also maximally diffracted. As expected then, we see in Fig. 5.10 that increasing the modulation voltage only increases distortion, whereas at lower modulation strengths we do not yet remove the  $1f_m$  signal as best as we can.

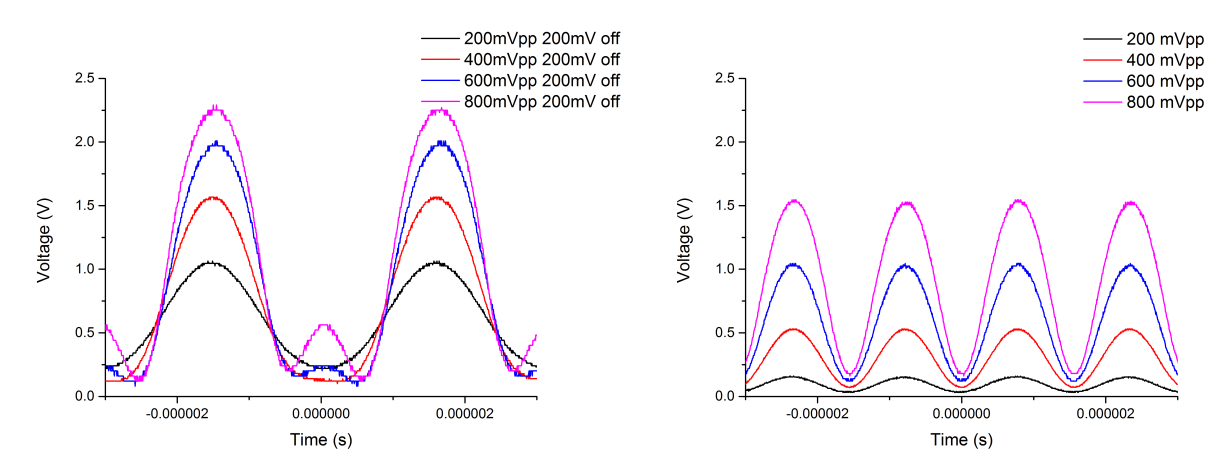


**Figure 5.7:** Oscilloscope images of output power of light leaving a modulated AOM measured with a photodetector. Left: with 200mV offset. We see a  $1f_m$  signal (black line) at 200mVpp modulation strength, which changes in a two-peaked signal (pink line) when the modulation is increased to 800mVpp, corresponding with an overmodulated signal described by Eq. (5.7). Right: without offset. We see a  $2f_m$  signal that increases as the modulation strength is increased.

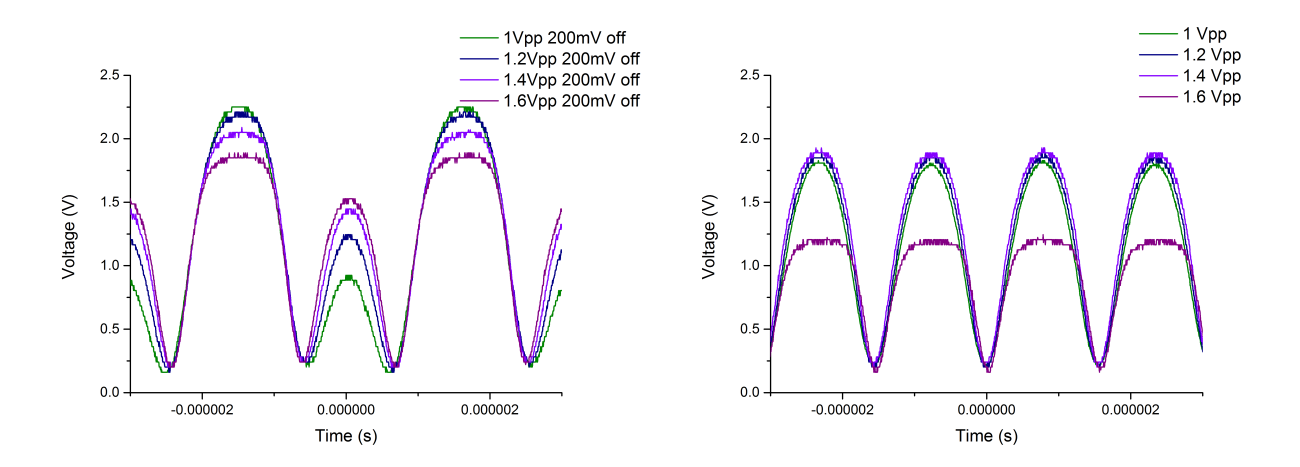


**Figure 5.8:** Oscilloscope images of output power of light leaving a modulated AOM measured with a photodetector. Left: with 200mV offset. The main peak decreases in size as the modulation strength is increased from 1Vpp to 1.8Vpp. The smaller peak however, increases. Right: without offset. The signal does not noticeably change in the range 1Vpp to 1.4Vpp. This means that increasing the modulation above 1Vpp no longer changes the amount of light diffracted into the first order. At 1.6Vpp, clipping starts to occur. The AOM cannot correctly respond to the driving voltage anymore.

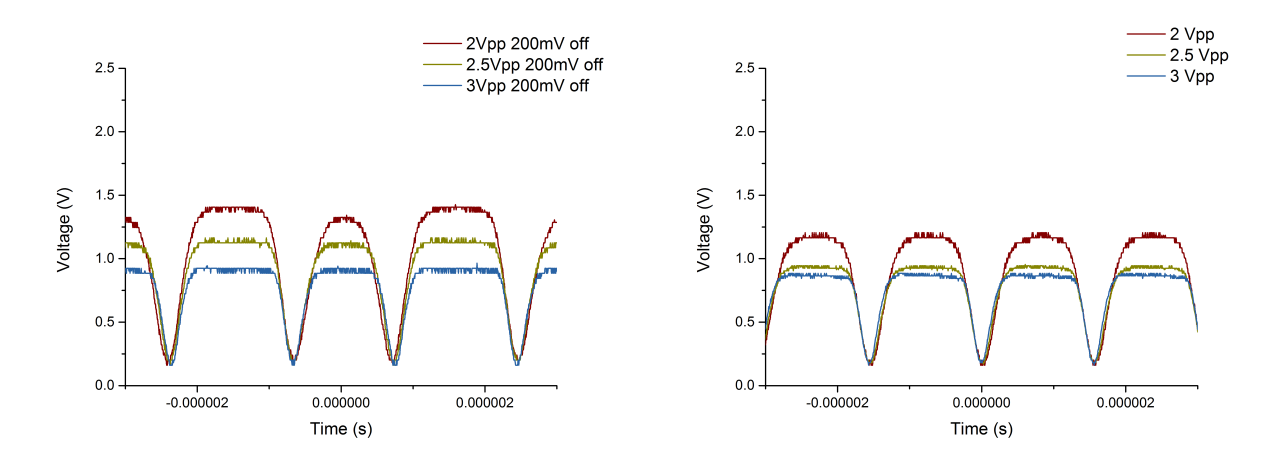


**Figure 5.9:** Oscilloscope images of output power of light leaving a modulated AOM measured with a photodetector. At this point the driving voltage is too high for the AOM to correctly process. Left: with 200mV offset. Now we see both peaks decrease in size as the modulation strength is increased. Right: without offset. The peaks decrease in size as the modulation strength increases, but not so much in the 2.5Vpp to 3Vpp as from 2Vpp to 2.5Vpp. This and the fact that at 3Vpp both with and without offset the signal has the same height seems to suggest that it will stabilize at some point and no longer decrease with increased modulation.

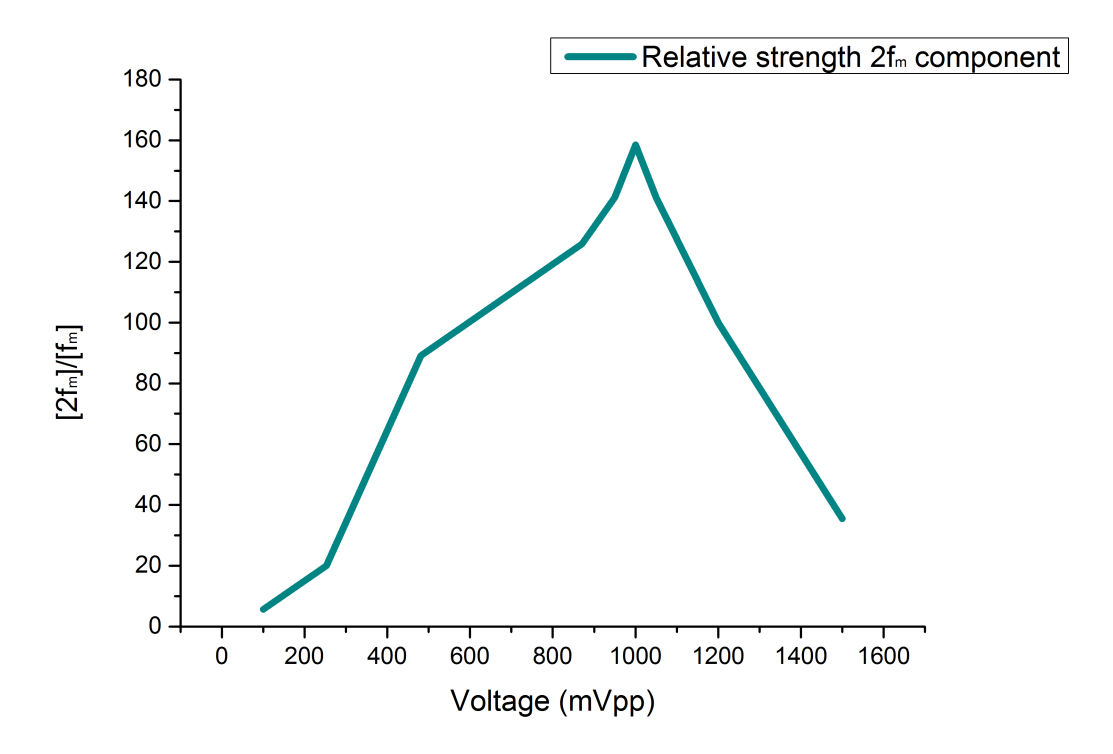


**Figure 5.10:** Size of  $2f_m$  component of the Fourier spectrum of the output waveform relative to the  $f_m$  component. The  $3f_m$  component was so small that we did not regard it in determining our eventual modulation strength. We see a peak at 1000 mVpp, suggesting that the sine wave is most suited for our purposed then. This coincides with the point of maximum intensity output.

### 5.4 Noise

In order to show that our setup is in principle capable of performing BAE measurement, we have to show that it can reduce noise at the mechanical resonance frequency, in the way explained in section 4.5. Since true back-action noise arising from shot noise is very small, this would not do for a first test. So we found a way to emulate back-action noise at a much greater intensity, so the effect would be noticeable long before we actually measure precisely enough to be limited by true back-action noise.

We achieved this by modulating the intensity of a laser at the mechanical resonance frequency. In this case, we modulated according to Eq. (5.7):

$$z(t) = A_l \sin(\omega_c t) + A_l A_m \sin(\Omega_m t) \sin(\omega_c t)$$

With  $A_l$  and  $A_m$  the amplitude of the laser and the modulation respectively. The resulting laser beam now has a Fourier component at  $\Omega_m$ . But back-action noise is, because it arises from random fluctuations, noise at all frequencies - white noise. It it just that we are most worried about noise precisely at the mechanical resonance. So to make sure that we influence the mirror in the right way, we will create white noise around the mechanical resonance frequency instead of just a delta spike at it. We do this by modulating the modulation signal in frequency. The theory behind this, is that a frequency modulated signal will have sidebands at the modulation frequency, but also at every higher order. The power that goes into these higher orders can be adjusted by increasing the modulation strength. The greater the amplitude of the modulation  $A_{fm}$ , the larger the bandwidth around the original

5.4 Noise 51

carrier wherein these sidebands have significant power. The modulation amplitude can be expressed as the peak divergence from the original carrier frequency ( $\Delta f$ ).

So we modulate the  $\Omega_m$  signal with a 1 Hz signal  $f_{fm}$ , and increase the modulation amplitude until all higher order sidebands in a bandwidth of 2 kHz contain significant power. This means that there is a max divergence of 1 kHz ( $\Delta f$ ) to either side of the carrier. An Agilent function generator provided this signal to the DC modulation input of the Toptica.

$$z(t) = A_l \sin(\omega_c t) + A_l A_m \sin(\Omega_m t) + \frac{\Delta f}{f_{fm}} \sin(2\pi f_{fm} t) \sin(\omega_c t)$$
 (5.8)

The resulting signal can be seen in Fig. 5.11.

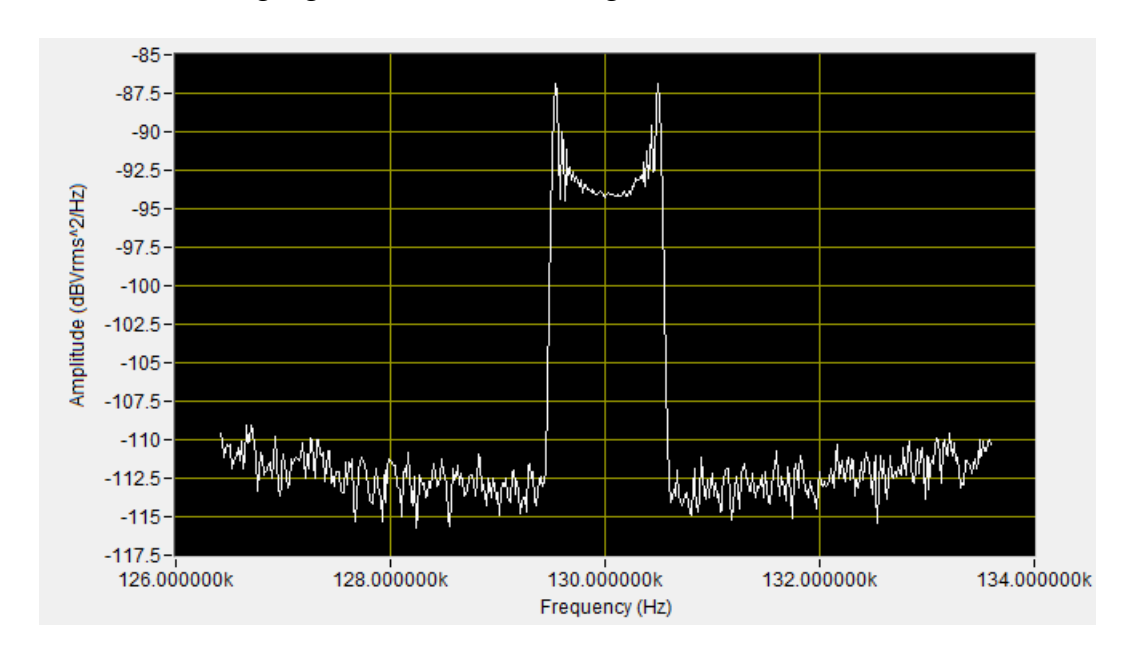


**Figure 5.11:** FFT of the noise injected in the cavity with the Toptica around a frequency of  $\approx 130 \text{kHZ}$  - the resonance frequency of mirror 7. We see that it gives the impression of a raised floor of white noise, though it actually consists of a series of delta spikes, spaced 1 Hz apart in a bandwidth of 2 kHz.

Sesults Results

### 5.5 Analysis

The measurements we eventually performed were FFT's (Fast Fourier Transforms) of the signal recorded by the photodetectors in transmission and reflection. Photodetectors measure intensity (power) per time f(t), which is Fourier transformed to power per (angular) frequency  $\hat{f}(\omega)$  according to the well known formula:

$$\hat{f}(\omega) = \frac{1}{\sqrt{2\pi}} \int_{-\infty}^{\infty} f(t)e^{it\omega}d\omega \tag{5.9}$$

I will analyze the results thus gathered by considering the Fourier Transform of the complete light field arriving at the photodetectors. I will however start by looking at the force acting on the mirror, in the case where we measure only with light at the cavity resonance frequency. In that case we expect to find the following frequency components of the light force acting on the oscillator (force, like intensity, is proportional to the square of the amplitude of the light field):

$$\mathscr{F}_t[\sin^2(\omega_c t)](\omega) = -\frac{1}{2}\sqrt{\frac{\pi}{2}}[\delta(\omega - 2\omega_c) + \delta(\omega + 2\omega_c) + 2\delta(\omega)]$$
 (5.10)

Meaning that the light will exert a constant radiation pressure proportional to  $A_c^2/2$  along with a fluctuating component  $A_c^2/2\sin(2\omega_c)$ , with  $A_c$  the amplitude of the light field of frequency  $\omega_c$ . This follows from the definition of the delta function, specifically:

$$\delta(x-a) = \begin{cases} 0, & \text{if } x \neq a \\ 1, & \text{if } x = a \end{cases}$$
 (5.11)

So that the light field acts upon the oscillator at all frequencies  $\omega$  for which one of the above delta peaks is non-zero. Of course, in reality, there is also the back-action force arising from the random fluctuations in the amount of photons arriving at the mirror every moment, which is what we are trying to evade. We neglect this for the moment, and ask what intensity is then measured at the photodetector, after this light has interacted with the mirror. The mirror phase modulates the light in the cavity, so that when it leaves, it will look like this:

$$\sin(\omega_c t + \sin(\Omega_m t)) \tag{5.12}$$

These phase modulations will result in a signal oscillating in intensity at the mechanical resonance frequency, which can be seen on the FFT. A good example of this is a measurement taken with only the PDH active on the reflection detector, see Figure 5.12. So far, so good; but when we actually measure we don't only send in a beam at cavity resonance. We send in the two sidebands of our measurement beam, the two PDH sidebands and the PDH beam at cavity resonance. And once in the cavity, the measurement sidebands will up- or down convert, forming two new beams in the cavity. Only if the sidebands are truly  $\Omega_m$  from cavity resonance they will form one beam at cavity resonance after scattering off the mirror, otherwise they, after exchanging exactly one phonon of energy, will be at a frequency  $\omega_c \pm (\omega_{aom} - \Omega_m)$ , with  $\omega_{aom}$  the modulation frequency of the sidebands. It is clear that only if  $\omega_{aom} = \Omega_m$ , the desired beam at  $\omega_c$  will be generated.

Ideally we are perfectly sideband resolved, so that the sidebands cannot enter except by up- or down conversion. Also the sidebands are exactly  $\Omega_m$  above and below cavity resonance, so that they form one beam at  $\omega_c$ . This will then be the only light in the cavity which is later transmitted to our photodetector, and we are again left with Eq. 5.12, yet without having caused back-action on the mirror. In practice however, the ideal case does not hold.

5.5 Analysis 53

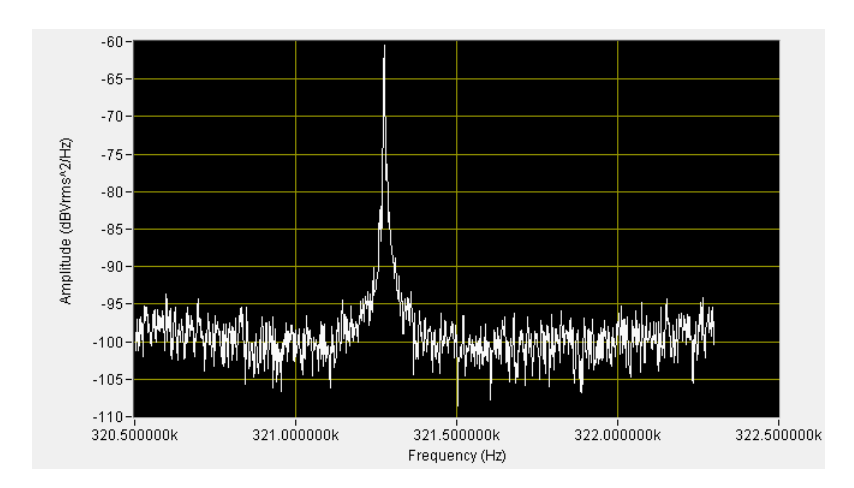


**Figure 5.12:** Measurement at  $\Omega_m$  with the reflection detector. Only the PDH laser is turned on.

The following analysis will provide a preliminary overview of the possible interferences in the cavity, which disturb our measurement. These disturbances will be mainly attributed to the fact that the above ideal conditions did not hold. I will then look at the actual measurements and show how some of these expected interferences have been found and what information we could gain by searching for others.

First we take the total system of electromagnetic waves in the cavity<sup>§</sup> (again disregarding back-action noise for the moment):

$$y(t) = A_c \sin(\omega_c t) + A_{aom} [\sin((\omega_c + \omega_{aom})t) + \sin((\omega_c - \omega_{aom})t)] + A_{sc} [\sin((\omega_c + \Delta\omega)t) + \sin((\omega_c - \Delta\omega)t)]$$
(5.13)

With amplitude  $A_c$  of the light at cavity resonance,  $A_{aom}$  the amplitude of the sidebands and  $A_{sc}$  the amplitude of the up- and down converted light. In this case,  $\Delta \omega = \omega_{aom} - \Omega_m$ . When we then want to calculate either the force acting on the mirror as a result of these beams, or the intensity recorded at the photodetectors, we take the square of this system:

$$y^{2}(t) = A_{c}^{2}[\sin^{2}(\omega_{c}t)]$$

$$+ A_{aom}^{2}[\sin^{2}((\omega_{c} + \omega_{aom})t) + \sin^{2}((\omega_{c} - \omega_{aom})t) + 2\sin((\omega_{c} + \omega_{aom})t)\sin((\omega_{c} - \omega_{aom})t)]$$

$$+ A_{sc}^{2}[\sin^{2}((\omega_{c} + \Delta\omega)t) + \sin^{2}((\omega_{c} - \Delta\omega)t) + 2\sin((\omega_{c} + \Delta\omega)t)\sin((\omega_{c} - \Delta\omega)t)]$$

$$+ 2A_{c}A_{aom}[\sin(\omega_{c}t)\sin((\omega_{c} + \omega_{aom})t) + \sin(\omega_{c}t)\sin((\omega_{c} - \omega_{aom})t)]$$

$$+ 2A_{c}A_{sc}[\sin(\omega_{c}t)\sin((\omega_{c} + \Delta\omega)t) + \sin((\omega_{c}t)\sin((\omega_{c} - \Delta\omega)t))]$$

$$+ 2A_{aom}A_{sc}[\sin((\omega_{c}t + \omega_{aom})t)\sin((\omega_{c} + \Delta\omega)t) + \sin((\omega_{c} - \omega_{aom})t)\sin((\omega_{c} + \Delta\omega)t)$$

$$+ \sin((\omega_{c}t + \omega_{aom})t)\sin((\omega_{c}t - \Delta\omega)t) + \sin((\omega_{c}t - \omega_{aom})t)\sin((\omega_{c}t - \Delta\omega)t)]$$

$$(5.14)$$

And then we perform a Fourier Transform like in Eq. 5.10 on the individual elements of this system. I've used the Fourier Transform calculator of Wolfram Alpha to calculate the frequency elements contained in this system and created a table of the results 5.2. I've grouped all terms of frequencies around  $2\omega_c$  because they are of no interest to us (their

<sup>§</sup>The PDH sidebands are so far from cavity resonance that they will not be taken into account here. I have also not included scattering from the PDH beam at resonance into the two sidebands at  $\omega_c \pm \Omega_m$ , for the sake of brevity. I have however included the unique terms arising from it in the table below 5.2.

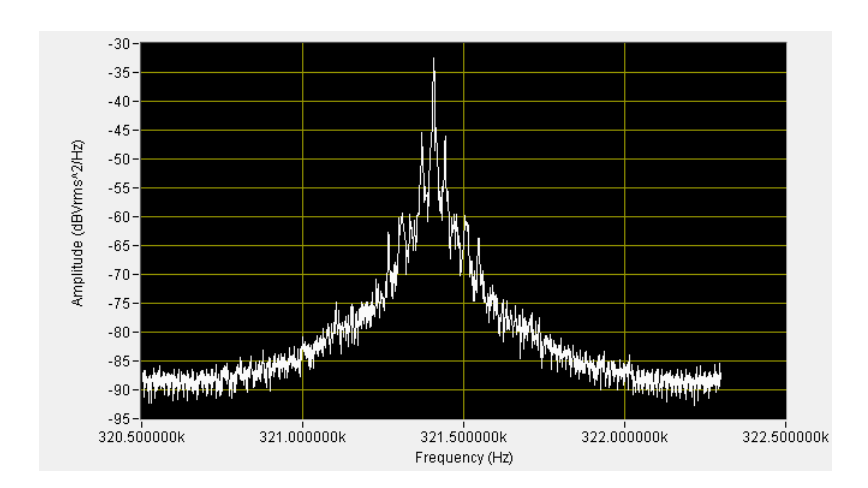


**Figure 5.13:** Measurement at  $\Omega_m$  in reflection with both the PDH and the measurement laser turned on. We see a signal much larger than the one we expect of the oscillator. This signal is due to interference between the reflected or leaked beam at the cavity resonance frequency  $\omega_c$  and the two sidebands at  $\approx \omega_c \pm \Omega_m$ .

frequency is much higher than any photodetector can record). I've also added terms arising from scattering of light at the cavity resonance into the sidebands at  $\omega_c \pm \Omega_m$ . The amplitude of this light is  $A_{scc}$ .

**Table 5.2:** Overview of all Fourier components of the light in the cavity. The numbers specify the relative weight of components in the Fourier spectrum.

	dc	$\Omega_m$	$2\Omega_m$	$\omega_{aom}-2\Omega_m$	$\omega_{aom}-\Omega_m$	$\omega_{aom}$	$\omega_{aom} + \Omega_m$	$2\omega_{aom}-2\Omega_m$	$2\omega_{aom}-\Omega_m$	$2\omega_{aom}$	$\approx 2\omega_c$
$A_c^2$	1/2										1/2
$\frac{A_{aom}^2}{A_{sc}^2}$	2/5									1/5	2/5
$A_{sc}^2$	2/5							1/5			2/5
$A_c A_{aom}$						1/2					1/2
$A_c A_{sc}$					1/2						1/2
$A_{aom}A_{sc}$		1/4							1/4		1/2
$A_{scc}^2$			1/2								1/2
$A_c A_{scc}$		1/2									1/2
$A_{aom}A_{scc}$					1/4		1/4				1/2
$A_{sc}A_{scc}$				1/4		1/4					1/2

Looking at Table 5.2, we expect signals at the modulation frequency of the AOM and at twice that frequency. Since both are caused by the sidebands created by the AOM modulation, either directly or through interference, we expect that these frequency components can only be found in the reflection if we are indeed sideband resolved. However, looking at Fig. 5.14 and 5.15 we see that at both the modulation frequency (5.14) and at twice that frequency (5.15) there always is a signal in transmission, suggesting that we are not sideband resolved: the sidebands can enter the cavity also without up- or downconversion. When we increase the frequency of the modulation we expect the signal at the transmission to decrease - which we indeed see, whereas the converse should happen in reflection. That we do not see this increase in reflection is probably due to the way PDH is set up. The signal from the photodetector is first mixed down and then passes a low-pass filter of around 200 kHz. All the FFTs we took are taken after this filter, so higher frequencies were cut off.

Focusing on the transmission detector, we see that the signal at the modulation frequency  $\omega_{aom}$  indeed resembles the signal at the reflection detector, yet smaller, see Fig. 5.14. The shape of the transmission signal suggests that it is actually formed of a series of small peaks, which are not properly distinguished in the FFT. The reflection signal however, seems to contain a very wide peak, upon which smaller peaks are present, see Fig. 5.15. These signals

5.5 Analysis 55

are probably caused by the interference terms  $A_c A_{aom}$  and  $A_{sc} A_{scc}$ . The first term describes the interaction between the sidebands and the PDH light at the cavity resonance frequency. The second term describes the interaction between the light that has been scattered after upor downconversion from the PDH light and up- and downconverted light of the sidebands. To check if this second term actually contributes we would have to measure at  $|\omega_{aom} - 2\Omega_m|$ . If a signal is present there it will also be present at  $\omega_{aom}$ .

The fact that we see a signal at  $\omega_{aom}$  at the transmission detector is worrying. If we would be properly sideband resolved than this signal should be gone. If we increase the modulation frequency we expect that the transmission signal will go down. We see in Fig. 5.14 that this happens, though even when  $\omega_{aom}=1200 \mathrm{kHz}$ , we still see a signal. That we still see a signal even if  $\omega_{aom}$  is well outside of the cavity linewidth can be explained by pointing out that the  $A_{sc}A_{scc}$  term can exist when the sidebands can only enter the cavity by up- and down-conversion. But that it still exists when the sidebands are at six times the cavity linewidth  $\frac{\omega_{aom}}{\kappa}=6$ , is hard to explain in this way.

That the reflection signal, which we would expect to increase as the transmission signal deceases, becomes smaller and even completely disappears when  $\omega_{aom}=900 \mathrm{kHz}$ , we can explain by pointing out that the reflection signal is mixed down and passes through a low-pass filter in the PDH setup. This filter was set at 200kHz during measurement, so it is to be expected that signals much higher than this frequency do not show on the FFT. We also see the noise floor perpetually decreasing as we look at higher frequencies. This is also the case in Fig. 5.15

The shape of the signal is also as of yet unexplained. The peaks are spaced  $\approx 50 \text{Hz}$  apart. They resemble some frequency- or phase modulated signal with a modulation index < 1 when the carrier is still the strongest signal and the sidebands are decreasing as they are spaced farther away from the carrier  $^{\P}$ . So perhaps it is caused by the PDH, which is perpetually changing the frequency of the laser on a timescale smaller than the cavity decay time, so the interference effects are still visible. It could also be caused by a ground loop.

When we turn our attention to Fig. 5.15, we see the FFT's in reflection (left) and transmission (right) at  $2\omega_{aom}$ . The only term in the interference pattern that could cause this is the  $A_{aom}^2$  term, the result of the two sidebands beating with each other. The transmission signal looks strange at first sight. It is much thinner than any other encountered signals. This could show that the AOM modulation is actually very precise, so that the broad peaks at the interference terms are caused by the light at the cavity resonance. This makes sense when we consider that the signal at twice the modulation frequency can only come from the  $A_{aom}^2$  interference, in which no other waves are present. It is independent of the laser frequency and thus corresponds with our suspicions of PDH of creating the shape of the interference pattern.

In reflection we see a smaller signal than in transmission, which again has to be attributed to the filter. Since we are now interested in signals at twice the modulation frequency, we see that the cut-off point comes sooner. Comparing the signals at  $\omega_{aom} = 900 \text{kHz}$  in Fig. 5.14 and at  $2\omega_{aom} = 1000 \text{kHz}$ , we see very comparable amplitudes (e.g. for the noise floor), suggesting that above 900kHz almost no signal is present anymore. We also see a lot of peaks in a space of a few kHz. These we cannot yet explain because the analysis does not provide

<sup>&</sup>lt;sup>¶</sup>This is not the case when the modulation index  $m_{fm} > 1$ . At  $m_{fm} = 2$  for instance, the carrier is reduced. And at  $m_{fm} = 4$  the first two sidebands are completely suppressed.

for interference terms so close to each other.

The last thing we did analyze are the FFTs taken at the mechanical resonance frequency, see Fig. 5.16. All the FFTs in the figure are taken in reflection, because there was no signal in transmission when the PDH functioned properly. Only when the feedback system failed to keep our measurement beam at a stable frequency did a transmission signal pop up. At the reflection however, we see in Fig. 5.16 that especially when  $\omega_{aom} > \Omega_m$  (at 500, 900 and 1200kHz) we see an excellent signal of the oscillator, increasing in size as the sidebands are spaced further from resonance. At 600kHz however, we suddenly see a interference pattern reminiscent of the one we see in Fig. 5.14, which seems to be an interference term. But when we plug in this value in the interference terms of Table 5.2, we do not find any other terms than the ones that always provide noise at the mechanical resonance ( $A_{aom}Asc$  and AcAscc). But since they are not present at 500kHz and neither at 900kHz, it is unlikely that they are suddenly so strong when the modulation is at 600kHz. We also see a lot of peaks near the mechanical resonance when  $\omega_{aom} < \Omega_m$ , at some 1kHz range. These are also not provided for by the terms in Table 5.2.

These last three observations are not yet explained. The transmission detector was not very well aligned because we focused on a mirror on the edge of the sample plane, but this cannot explain why we see no signal at the mechanical resonance frequency. After all, with only a very weak PDH beam we see an excellent signal in reflection. And we've performed other quality measurements using the transmission detector (but no PDH), so it is certainly strange. That some signal is visible when PDH falls out of lock seems to suggest that the measurement beam is of another frequency than the PDH laser and only enters the cavity (perhaps with only one sideband) when the PDH laser no longer does that. But this does not explain why we see nothing with only the PDH present. But whether both lasers are actually tuned to resonance, can be investigated by searching for the interference terms of Table 5.2. If they are not found where we've predicted them it might suggest that this difference of frequency, perhaps due to the AOMs, is indeed the case. And the strange signals when  $\omega_{aom} < \Omega_m$  and  $\omega_{aom} = 600 \text{kHz}$  are also still a mystery.

We can also use Table 5.2 to understand what it means for the ideal conditions (being side-band resolved and  $\omega_{aom}=\Omega_m$ ) to hold. In that case  $A_{aom}$  and  $A_{scc}$  will become zero inside the cavity (they cannot enter), and the remaining oscillating terms of  $A_{sc}^2$  and  $A_cA_{sc}$  will become dc signals (since  $\omega_{aom}=\Omega_m$ ). So it is immediately clear how important it is to fulfill these conditions: without them there is noise everywhere. Even at the mechanical resonance the interference between the sidebands and the up - and down converted light creates noise. If this term has a larger amplitude than the back-action noise from one laser, we have essentially made our measurement *more* imprecise. And this only becomes worse if  $\omega_{aom}=\Omega_m$ . In this case the up - and downconverted light is at the cavity resonance, but now the interference between the sidebands and this light is twice as large at the cavity resonance (the  $A_{aom}A_{sc}$  term with the condition  $\omega_{aom}=\Omega_m$ ). And since the PDH also injects light at the cavity resonance, a second noise term at  $\Omega_m$  will be created (the  $A_cA_{aom}$  term with the condition  $\omega_{aom}=\Omega_m$ ). It may therefore not be surprising that we were not yet able to perform a measurement of the oscillator when  $\omega_{aom}=\Omega_m$ .

5.5 Analysis 57

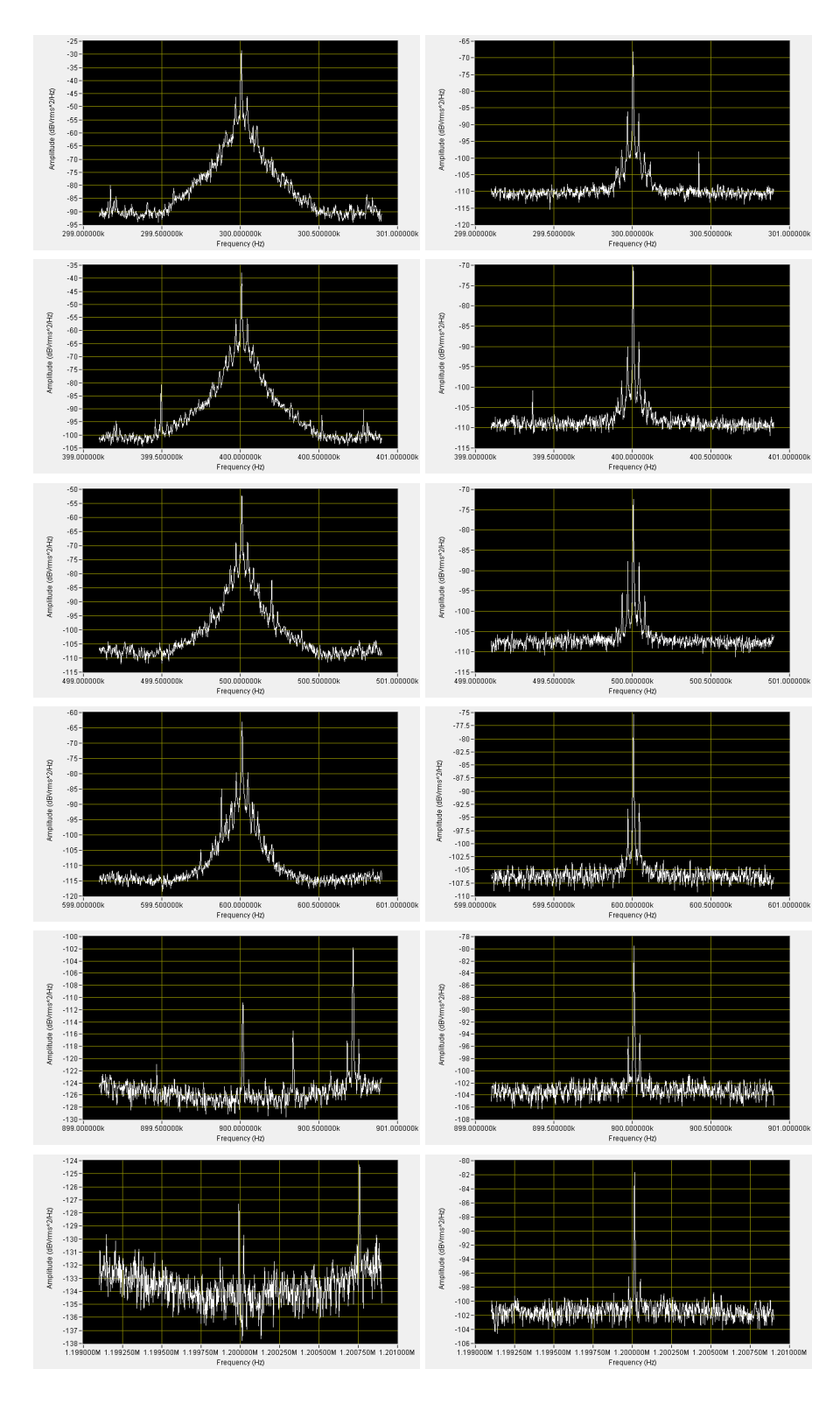


**Figure 5.14:** Left: reflection. Right: transmission. From top to bottom: FFT at 300, 400, 500, 600, 900 and 1200 kHz, with the AOM modulation always at the same frequency. We expect these signals to be caused by the interference between light at the cavity resonance and the sidebands created by the AOMs. Therefore we attribute the decreasing amplitude in reflection to a filter effect which is due to the PDH method; whereas we attribute the decrease in transmission to more of the sidebands being rejected because of the cavity bandwidth.

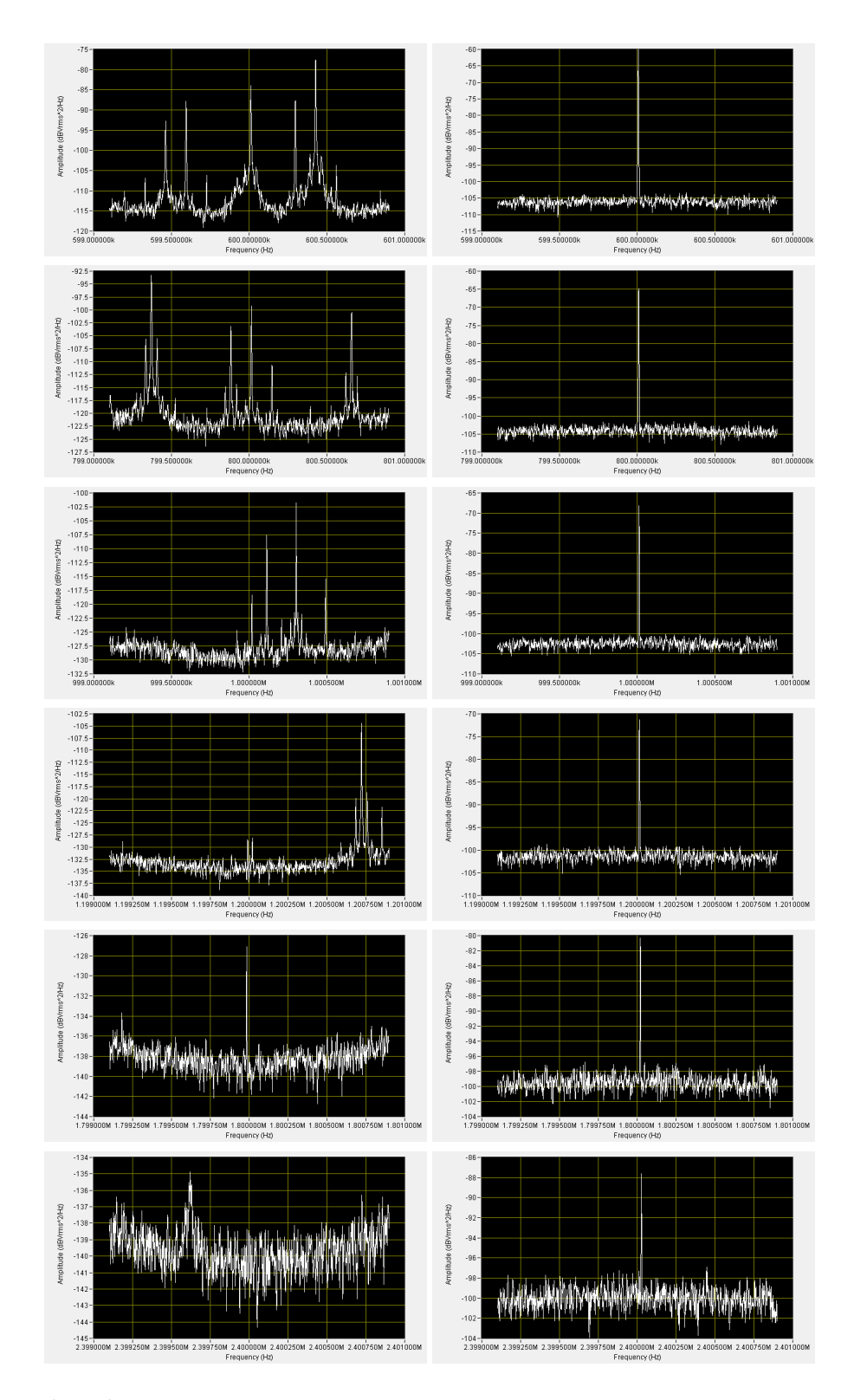


**Figure 5.15:** Left: reflection. Right: transmission. From top to bottom: FFT at 600, 800, 1000, 1200, 1800 and 2400 kHz, with the AOM modulation always half that frequency. We expect these signals to be caused by the sidebands of the AOM. Therefore we expect that they are larger in the reflection than in transmission. Though again, because of PDH filtering we cannot compare the height of the two signals. Also, the transmission peak is very small and does not look like a real signal, even though it is persistent. There are multiple peaks in reflection, spaced  $\approx 1 \text{kHz}$  apart.

5.5 Analysis 59

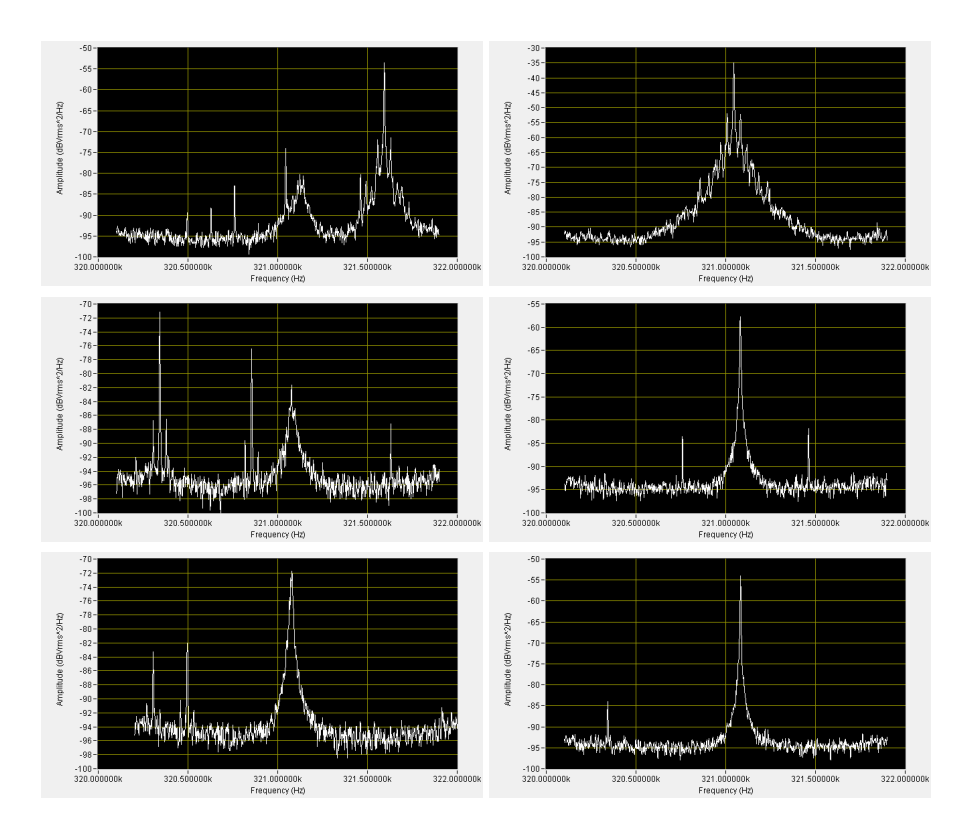


**Figure 5.16:** FFTs taken at 321 kHz, approximately the mechanical resonance frequency. From from top to bottom and then from left to right: 300, 400, 500, 600, 900, 1200 kHz AOM modulation. We can see that the signal of the oscillator becomes larger as the modulation increases. Only at 600 kHz there is a strange break in the pattern as a peak reminiscent of the interference between the AOM sidebands and the cavity resonance frequency suddenly overwhelms the oscillator signal.

### 5.6 The Next Steps

We do not yet completely know what happens in the cavity when the PDH and the measurement beam are both present. We can however outline the next steps that can be taken to gain more insight in the problem and to improve the current setup.

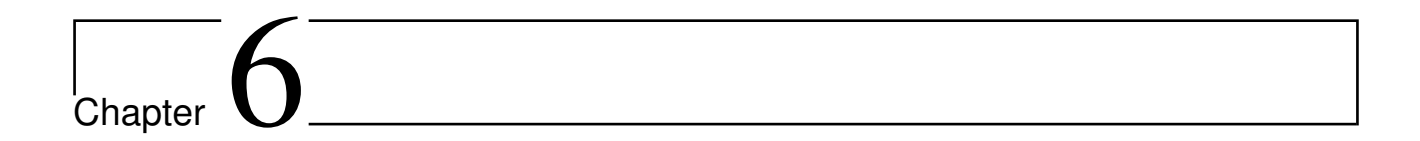
- 1. I believe it is possible to make a FFT of the reflection signal before it passes the low-pass filter. This would require no more than the switching of two cables and enable us to actually compare the transmission and reflection signal.
- 2. We can investigate other interference terms as written down in Table 5.2. This would help us understand whether this picture of the lightfield in the cavity is accurate or should be rejected.
- 3. We should ascertain that the transmission photodetector is correctly aligned. During these measurements we focused on a sample in the corner of the sample plane and possibly only a small part of the light transmitted reached our detector.
- 4. We should use two lasers, and make sure that the PDH laser is located one free spectral range ( $\approx 3GHz$ ) away from our measurement laser, so that the interference between PDH light at the cavity resonance and the sidebands of the measurement beam can no longer interfere in the kHz range. This would require a phase lock loop to make sure that the measurement laser follows the PDH laser.
- 5. We need a better sample. Though, if perfectly aligned these samples should do fine. But we cannot be sure yet if better alignment is possible with our precision (no motors, everything done by hand).
- 6. A question that would be worth answering is: what is the influence of the linewidth of the oscillator on our measurements? The smaller it is, the more difficult it becomes to correctly modulate the AOM so that the up- and down converted beam overlap. On the other hand, a very wide linewidth could result in unwanted interference in a broader range. The working assumption is thus: it is easier to achieve BAE with a low-Quality oscillator, but to do it right, we need one with a very small linewidth.
- 7. We have to find out what causes the interference at  $\approx 50Hz$  which is visible at a lot of the peaks. Possibly it is created by the AOM because of a mains hum which sneaked inside the system somehow. Or it is a frequency modulation either stemming from the AOMs or from the PID controller for PDH.
- 8. We have to find out what causes the interference patterns at a few kHz from each other. For instance, we see in Fig. 5.16 that when  $\omega_{aom} < \Omega_m$  (first two pictures) there are several peaks visible that are at approximately 1kHz distance. There is as of yet nothing in the model we've used that can account for this.
- 9. It is possible that a lot of information can be gained by finding out what causes the peak at 321kHz when we modulate the AOMs with 600kHz. It is a reproducible result and we should expect to find a definite interference term causing it. If it is found it can be used to construct a better model.

There are also some elements of the setup that we've already created but have not yet been able to use.

5.6 The Next Steps 61

• An electronic feedback system made by Kier Heeck to make sure that both AOMs can be locked to a certain frequency distance between them. In this way we can move the two sidebands so that they are not centered around the cavity resonance anymore. This can be used to show that BAE works. The system has been tested successfully.

- A way to modulate the phase of our amplitude modulation. This is crucial for BAE, so you can select only one quadrature to measure. It has not yet been tested.
- We have not yet measured with the noise laser and the PDH laser and the measurement beam. We are not sure if it will disturb PDH. We aim to solve this issue by making sure that the noise is at least a free spectral range removed from the PDH beam.

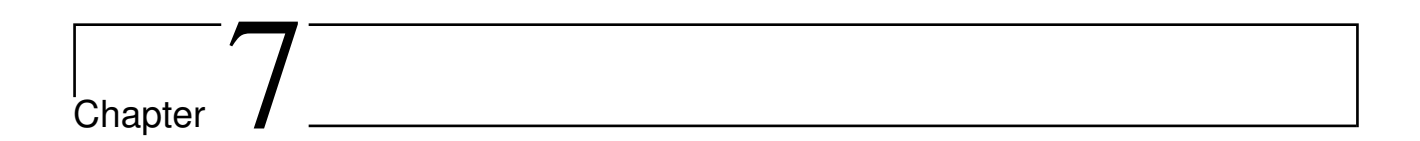


# Conclusion

The goal of this Bachelor project was to build a setup capable of performing classical backaction evading measurements. Though we did not yet perform such measurements, a lot of the preliminary steps have already been taken.

We have designed an optical bench to hold our sample and shown that it can be aligned to form a cavity. The finesse and the mechanical resonance frequency of samples have been measured. We have created two optical drives spaced one mechanical resonance frequency above and below the cavity resonance frequency. This is done by modulating the amplitude of our laser with an AOM. Also, we have created a noisy laser emulating back-action noise using a combination of frequency- and amplitude modulation. We have included a Pound-Drever-Hall feedback lock in our system and shown that we can measure while the feedback lock is turned on. We have measured the light reflected from and transmitted through the cavity using photodetectors and analyzed the Fast Fourier Transforms of the signals from the photodetectors. From this we conclude that we are not sideband resolved enough. We therefore need another sample or better alignment. We should also detune the feedback lock from our measurement laser.

This Bachelor thesis also aimed to provide an overview of the most important elements of the setup and theory necessary for the continuation of this project. I hope that someone will be able to use it for that purpose.



# Acknowledgments

I would like in the first place to thank Gesa Welker, who guided me and helped me during the whole course of this project. I am further indebted to Frank Buters and Hedwig Eerkens for giving me tons of practical advice on aligning and the use of apparatus and showing me in general what it means to work in a lab.

This thesis would also not have been possible without Harmen van der Meer, who built the optical bench that we've used and Kier Heeck, who gave technical advice and built some of the devices necessary for the next steps.

And finally I would like to thank Dirk Bouwmeester for making this whole project possible and showing confidence in me.



# Appendix

# 8.1 Appendix 1: Alignment of the Cavity

This section contains a list of the steps we followed to align the cavity. It is essentially the same procedure as written down by Frank Buters and Hedwig Eerkens, who are working with a similar optical bench, and which I initially followed. I have chosen to write my own section and not copy their procedure here, because my version incorporates the tips and tricks I learned from them during the alignment procedure and not just the steps one should follow.

- 1. Use a red laser so that you can see the light during the first steps of alignment. The lenses are of course not attuned to red light, but this is not necessary for these first steps.
- 2. Replace the large cavity mirror with a pinhole the bench is designed to make this switch easy and make sure that the red laser goes through the pinhole using the first periscope mirror the one closest to the fiber. You can place the fiber at the desired distance from the lens so that the beam is small enough. Do not touch the attacube during this stage.
- 3. When the beam has entered the cavity, it reflects from the small mirror(s). Roughly align the sample holder so that this first reflection also goes through the pinhole. This is quite difficult to see, because of the diffuse reflections around the pinhole. The best way is to make the incoming beam larger, so that the beam is smallest after it has reflected and you see a clear point which you can control. When you can't see it, it is wise to first turn the sample plane till it is visible, so you can track it with your eye. All of this cannot be done to great precision, but it suffices for now.

  Note: make sure that the screws of the big cavity mirror and the sample plane are at the beginning of the procedure somewhere in a middle position, so that you later have maximum freedom to adjust them. Also try to start out with both roughly parallel, if the sample then turns out to be tilted, you can adjust accordingly.
- 4. Now switch to the infrared laser and remove the second mirror the one closest to the cavity. Make sure that you have some free space in the direction of the beam which reflects from the first mirror off the table. Use a card which makes the light visible and try to make the beam collimated by moving the mirror holder. In principle it should be in the right position as near to the lens as possible. It can be useful to make sure that the attacube is somewhat in its middle position, so that you later have maximum

68 Appendix

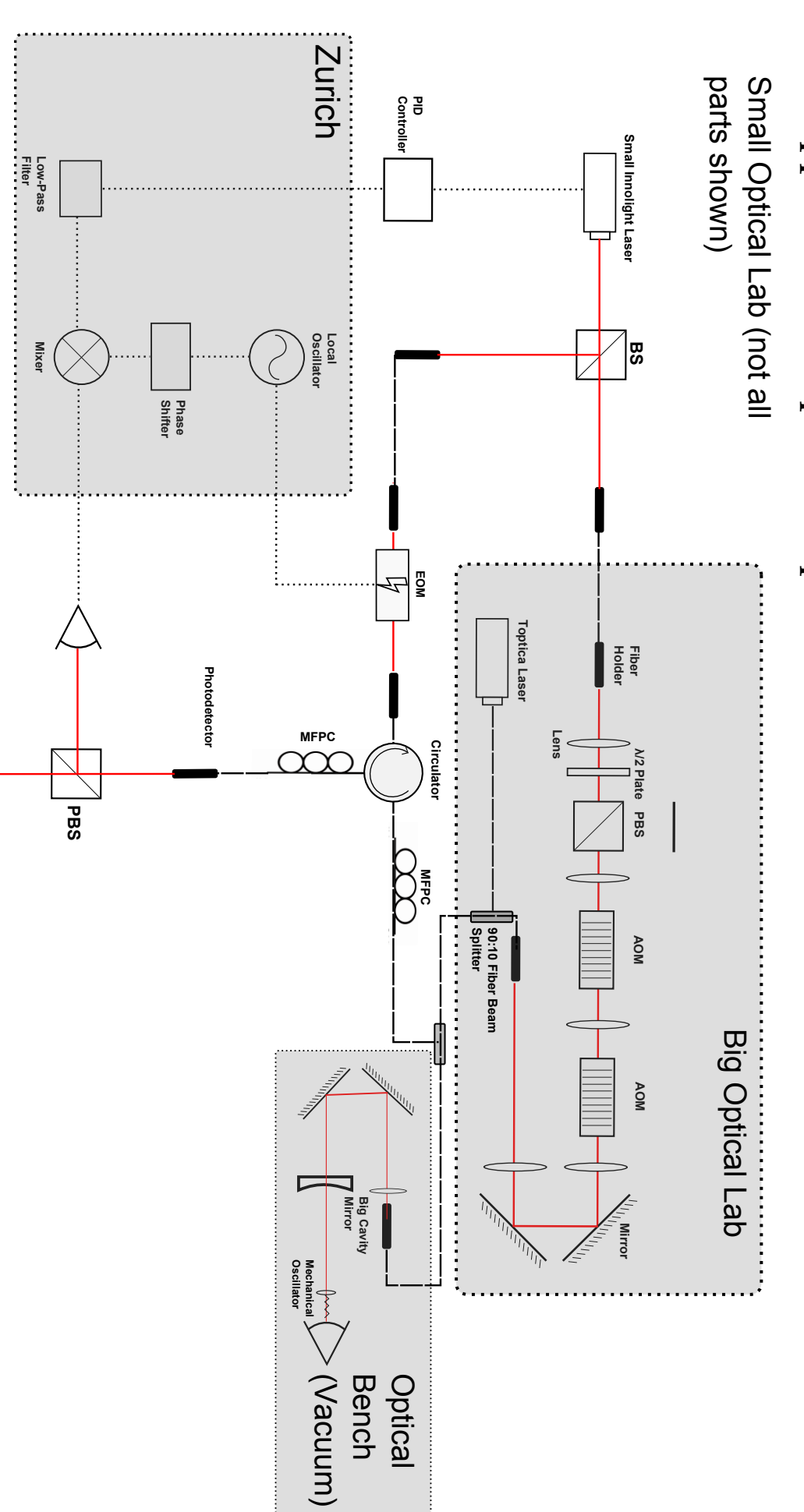
freedom in both directions during finetuning. When you are convinced that the beam is roughly collimated, you can place the second mirror back in.

- 5. Replace the pinhole with the big mirror. To align the cavity you need something able to see the position of the laser beam on the sample plane. Therefore place a CCD camera with an additional external lens behind the sample plane. After some maneuvering, which will become easier with time, one gets a clear image of all the samples (16 in our case) in the sample plane, along with a bright spot signaling the position of the laser. All of this can best be done in the dark, else the laser will be invisible on the TV connected to the camera. But if you want to see all samples at once you need more light than the laser provides. A small lamp is therefore useful to have nearby. Once the camera is focused on the samples in such a way that you can clearly see their arms, it is important to check which samples can be used. After you have memorized the positions of the good samples, you can turn off the lamp and use the laser illuminating a small region only.
- 6. You will notice that adjusting orientation of the second periscope mirror moves the bright spot of the laser across the sample plane. You can use this to aim for the center of the small mirror you have chosen. There should also be another spot, somewhat less bright and possibly of a different size (this means that your incoming beam is not perfectly mode matched to the cavity yet move the attacube until they are about the same size) as your main spot. This is the first reflection, and you want to make sure that it also hits your chosen sample. To move this spot you can use the screws of the big mirror. Notice that moving with the second periscope mirror moves both spots, whereas moving with just the big mirror only moves the reflection. The idea is that because the incoming beam goes through the middle, the orientation of the big mirror does not matter for how it enters the cavity. So you play around with both until they overlap on the sample.
- 7. The next thing is to make sure that the cavity has the right length. If your original beam and the reflection both fall on the sample, yet are still clearly visible in the area around the mirror, they are probably too wide. You have to try by increasing and decreasing the length a bit (for instance by adjusting all screws of the big mirror by the same amount, say: one turn) to get it right. Then you should see a bright spot in the middle of the mirror and as little as possible but still some light as a halo around it.
- 8. To find out how good your cavity is you need something more accurate than your eye, for this you use photodetectors, registering the transmitted and reflected light from the cavity. The transmission detector will have to compete with the CCD, therefore place a beamsplitter between the CCD and the lens, so that 50 percent of the light can be caught with the photodetector. It might be necessary to switch to the red laser to make sure that it is at the right position, for the transmitted infrared beam might be too weak to see. The reflected light you have to separate from the incoming light with the circulator before you can measure. The third fiber of the circulator can then be immediately attached to a photodetector.
- 9. Both photodetectors are linked to an oscilloscope so we can see their response. Using Digilock scan the laser frequency over at least one free spectral range, so that if you have a cavity it will show up. You want to see a peak in transmission at the same time that a dip in the reflection occurs.
- 10. Now you can reiterate all the previous steps, because it is probably the case that as a result of the first alignment of the cavity the incoming light no longer goes through the

middle of the big mirror. So you should bring back the pinhole and check whether that is the case. Since at least the length of the cavity is now about right, every iteration will be faster than the previous.

70 Appendix

# 8.2 Appendix 2: Complete Setup



etc., I did not include in the drawing because I did not build or align them. could be split into a part containing PDH light and a part containing measurement light. It was important that they did not interfere on the PDH photodetector. Our results show that we did not fully succeed in this. Some parts in the small optical lab, including beam stops, fiber holders, mirrors transmission results. The MFPC are Manual Fiber Polarization Controllers, which we used to make sure that the light that was reflected from the cavity, Figure 8.1: Complete setup. The part labeled 'Zurich' is a Zurich Instruments Lock-in Amplifier. We used another one in the big optical lab for the

# 8.3 Appendix 3: Sample Plane and Mirror

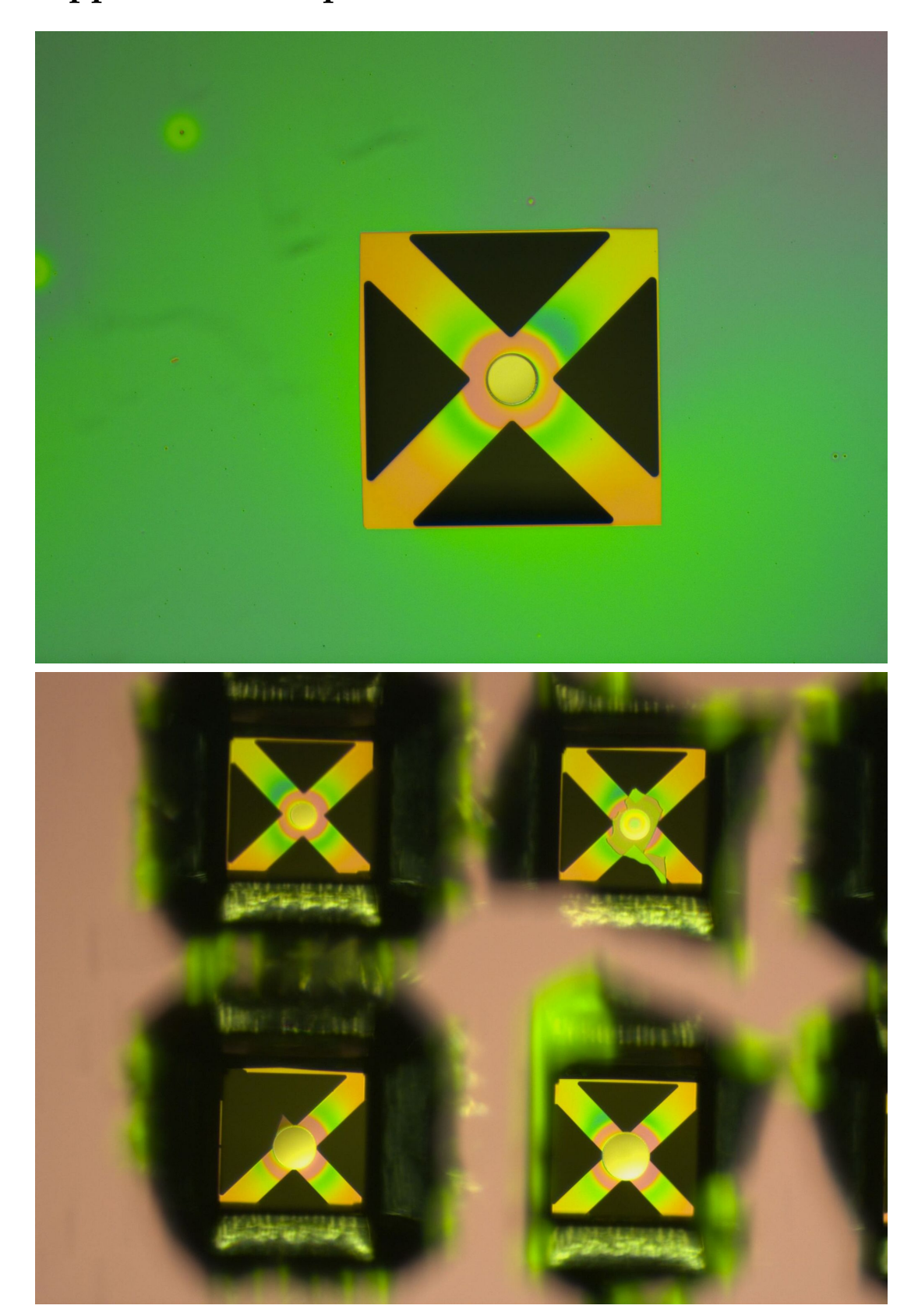


**Figure 8.2:** Top: Picture of mirror 4. Bottom: Picture of part of the sample plane. The whole plane held 16 mirrors.

# References

- [1] C. M. Caves, K. S. Thorne, R. W. P. Drever, V. D. Sandberg, and M. Zimmermann. On the Measurement of a Weak Classical Force Coupled to a Quantum-Mechanical Oscillator .1. Issues of Principle. *Reviews of Modern Physics*, 52(2):341–392, 1980. WOS:A1980JS02600003.
- [2] D. F. Walls and G. J. Milburn. *Quantum Optics*. Springer Science & Business Media, January 2008.
- [3] M. F. Bocko and R. Onofrio. On the measurement of a weak classical force coupled to a harmonic oscillator: experimental progress. *Reviews of Modern Physics*, 68(3):755–799, July 1996.
- [4] W. Marshall, C. Simon, R. Penrose, and D. Bouwmeester. Towards quantum superpositions of a mirror. *Physical Review Letters*, 91(13):130401, September 2003. WOS:000185573700001.
- [5] A. A. Clerk, F. Marquardt, and K. Jacobs. Back-action evasion and squeezing of a mechanical resonator using a cavity detector. *New Journal of Physics*, 10:095010, September 2008. WOS:000259616300009.
- [6] M. J. Weaver, B. Pepper, F. Luna, F. M. Buters, H. J. Eerkens, G. Welker, B. Perock, K. Heeck, S. de Man, and D. Bouwmeester. Nested trampoline resonators for optomechanics. *Applied Physics Letters*, 108(3):033501, January 2016.
- [7] M. Aspelmeyer, T. J. Kippenberg, and F. Marquard. Cavity optomechanics. *Reviews of Modern Physics*, 86(4):1391–1452, December 2014. WOS:000347201400001.
- [8] D. Kleckner, I. Pikovski, E. Jeffrey, L. Ament, E. Eliel, J. van den Brink, and D. Bouwmeester. Creating and verifying a quantum superposition in a microoptomechanical system. *New Journal of Physics*, 10:095020, September 2008. WOS:000259616300019.
- [9] E. D. Black. An introduction to Pound-Drever-Hall laser frequency stabilization. *American Journal of Physics*, 69(1):79–87, January 2001. WOS:000166018200011.
- [10] K. Karrai, I. Favero, and C. Metzger. Doppler optomechanics of a photonic crystal. *Physical Review Letters*, 100(24):240801, June 2008. WOS:000256942400013.
- [11] A. Schliesser, R. Rivière, G. Anetsberger, O. Arcizet, and T. J. Kippenberg. Resolved-sideband cooling of a micromechanical oscillator. *Nature Physics*, 4(5):415–419, May 2008.
- [12] V. B. Braginsky, Y. I. Vorontsov, and K. S. Thorne. Quantum Nondemolition Measurements. *Science*, 209(4456):547–557, August 1980.

74 References

[13] F. Marquardt, J. P. Chen, A. A. Clerk, and S. M. Girvin. Quantum Theory of Cavity-Assisted Sideband Cooling of Mechanical Motion. *Physical Review Letters*, 99(9):093902, August 2007.

- [14] F. L. Pedrotti and L. S. Pedrotti. *Introduction to Optics*. Prentice Hall, January 1993.
- [15] D. Kleckner, B. Pepper, E. Jeffrey, P. Sonin, S. M. Thon, and D. Bouwmeester. Optome-chanical trampoline resonators. *Optics Express*, 19(20):19708–19716, September 2011. WOS:000295373800096.
- [16] Frenzel Jr, L. E. *Principles of Electronic Communication Systems*. McGraw Hill, 3rd edition, 2008.